EXPERIMENTAL INVESTIGATION OF THE FATIGUE BEHAVIOUR OF NATURAL RUBBER UNDER DIFFERENT LOADING AND ENVIRONMENT CONDITIONS

CAN ZHANG

A DISSERTATION SUBMITTED TO THE FACULTY OF GRADUATE STUDIES
IN PARTIAL FULFILMENT OF THE REQUIREMENTS
FOR THE DEGREE OF
MASTER OF SCIENCE

GRADUATE PROGRAM IN MECHANICAL ENGINEERING
YORK UNIVERSITY
TORONTO, CANADA

APRIL 2021

Abstract

Natural rubber is widely used in industrial fields owing to its good elasticity and ductility. It is important to study the fatigue behaviour of rubber because it affects the service life of rubber products. The objectives of this study were to (1) develop a new protocol to understand how deformation, temperature, frequency, and aging impact natural rubber fatigue behavior; (2) investigate the relationship between the number of fatigue life cycles and the applied load; and (3) evaluate the macromorphology of the fracture area, and observe the crack propagation rate and direction. The dynamic fatigue process of rubber materials can generally be divided into three stages: stress softening, crack nucleation, and crack growth. When the frequency is below 5Hz and the deformation is 25% strain level, the crack growth rate is stable, the fracture interface is flat, and the fatigue life is long. Moreover, temperature influences include the effect of the environmental temperature and the heat generated by the self-heating of rubber. Thermal aging caused by high temperature will reduce the fatigue life of rubber, which is one-tenth of the fatigue life of unaged samples. The results of this work can be used to inform the future design, production, and application of rubber parts so that the emergence of rubber fatigue can be appropriately prevented or delayed.

Acknowledgements

Foremost, I would like to express my sincere gratitude to my supervisor Dr. Aleksander Czekanski for the continuous support of my master's study and research, for his patience, motivation, enthusiasm, and immense knowledge. His guidance helped me in all the time of research and writing of the thesis. I could not have imagined having a better supervisor for my master's study. Besides my supervisor, I am grateful to the Natural Sciences and Engineering Research Council of Canada (NSERC) for providing important financial support to my research.

I would like to thank to my colleagues, for their encouragement and support. Without their help I would not be able to succeed in my research. My sincere thanks also go to technicians for helping me adjust experiment equipment.

Finally, I would like to thank my dear family: my parents and grandparents for supporting me spiritually through my life. Thanks to my friends in Canada for their help in life.

Contents

List of Tables

List of Figures

Chapter 1: Introduction

1.1 Background

Owing to its superior elasticity and large deformation capacity, rubber is widely used in the manufacturing of machinery, automotive parts, and diverse components for many other industries, making it ideal for applications as varied as vibration isolators, belts, seals, medical devices, and more [1]-[2]. Fatigue behaviour is an important characteristic that affects the life of rubber products. Mechanical structures containing rubber dampers are subjected to various forms of loading during their normal service life and are expected to run reliably for several years. Therefore, it is essential to evaluate the fatigue life of rubber dampers under different conditions to determine how the parts will perform.

Various tests are used to evaluate the performance of rubber components, including those that measure heat resistance, fatigue resistance, and aging resistance in a complex working environment. This working environment has stringent requirements to ensure the comprehensive performance of rubber and a long service life. The fatigue failure of rubber refers to the phenomenon whereby the mechanical properties of the material itself are reduced under periodic deformation or cyclic loading [2]. Crack nucleation and crack growth are two common approaches to measuring rubber fatigue [4]-[5]. At the microlevel, these approaches focus on predicting the position of the appearance of the first crack in a rubber sample and the growth of existing cracks or flaws [6]-[7]. The most obvious feature

is the appearance of cracks on the surface of rubber products. When the crack grows to a certain length, the rubber product completely fails. Therefore, it is important to explore damaging processes in order to predict fatigue life.

Because of its large stretch ratio and high resilience, natural rubber is used extensively. Nearly 50% of the material used in high-performance tires for airplanes, race cars, and public transport vehicles consist of natural rubber [8]. Since natural rubber products have been so widely used under cyclic loading conditions, this study focuses on natural rubber material.

1.2 Motivation for the study and objectives

The objectives of this experimental investigation into the fatigue behaviour of natural rubber were to:

1. Investigate a protocol of rounded samples to capture how strain level, temperature, frequency, amplitude, and aging impact the fatigue behaviour of natural rubber.
2. Determine the relationship between the number of fatigue life cycles and the applied load for various loading and environment conditions.
3. Evaluate the macromorphology of the fracture area and observe the rate and direction of crack propagation.

1.3 Outline

The thesis includes five chapters. Chapter 1 contains the introduction and background of the study. Chapter 2 provides a review of the literature related to existing rubber fatigue studies and current knowledge gaps. Chapter 3 introduces the test material and describes the experimental method. Two kinds of results are presented and discussed in chapter 4: fatigue life analysis and observation of fracture characteristics. Finally, chapter 5 summarizes the implications of the work performed, identifies the original contributions, and outlines suggestions for future work.

Chapter 2: Literature Review

This chapter describes the development and application of natural rubber and the current situation of rubber fatigue research, including research on crack initiation and crack growth, and the influence of some external factors on rubber fatigue behavior.

2.1 Material

Natural rubber refers to the elastic solids made from natural rubber latex collected from Brazilian rubber trees through coagulation, drying, and other processing procedures [9]. Natural rubber is a natural polymer with *cis*-1,4-polyisoprene as the main component. Its molecular formula is $(C_5H_8)_n$ [9]. Natural rubber has a hydrocarbon content of over 90%, but also contains a small amount of protein, fatty acid, sugar, and ash [10].

In terms of physical properties, natural rubber has high elasticity at room temperature, slight plasticity, high mechanical strength, low hysteresis loss, and low heat generation during multiple deformations. Hence, natural rubber also has good flex resistance. As a nonpolar material, natural rubber has good electrical insulation properties [10].

Natural rubber also has many favourable chemical properties. Because of the unsaturated double bond in *cis*-1,4-polyisoprene, natural rubber has high chemical reactivity [11]. For instance, light, heat, ozone, radiation, flexural deformation, and metals such as copper and

manganese can promote the aging of rubber. The major weakness of natural rubber is its inability to age. However, natural rubber that contains antiaging agents sometimes does not show much change after 2 months of exposure to the sun and can still be used as usual after 3 years of storage in a warehouse.

Given these physical and chemical properties, natural rubber has a wide range of applications [12]. For example, it is found in everyday items such as rain boots, hot water bottles, and elastic bands; medical items such as surgical gloves and biomembranes; tires and conveyor belts; acid- and alkali-resistant gloves used in industry; drainage and irrigation hoses and ammonia bags for agriculture; air-sounding balloons used in meteorological measurement; sealing and anti-vibration equipment used in scientific experiments; aircraft, tanks, artillery, and gas masks used in national defense; and even high-tech products such as rockets, artificial earth satellites, and spacecraft.

2.2 Current studies

2.2.1 Fatigue crack initiation and growth approaches

The material fatigue failure process can be roughly divided into two stages: crack nucleation and crack propagation (Figure 2.1). The crack nucleation stage includes the microcrack growth period, and the crack propagation stage includes the macrocrack growth period and the instantaneous fracture period. Investigations of crack nucleation focus on

predicting the position of the appearance of the first crack in a rubber sample and the growth of existing cracks or flaws [13]. The maximum principal strain and strain energy density are the two main parameters of the crack nucleation stage [4]. The maximum principal strain is usually used to characterize the nucleation life of a crack in rubber [14]. From the late 1850s to the early 1960s, after some progress in the theoretical research on the fracture mechanics of rubber, strain energy density gradually became a parameter for predicting crack nucleation life [15]. Strain energy density measures the energy release rate of internal defects. Under certain conditions, the energy release rate is proportional to the product of strain energy density and crack size. Therefore, the strain energy density can evaluate the energy release rate.

There are two theories about the formation of microcracks. One is the molecular motion theory [6]. According to this theory, under the action of a dynamic load, the stress is concentrated on the weak chemical bond of the rubber and thus causes microcracks. Another theory is Griffith's theory, which is commonly used in the analysis of metal fractures [17]. As early as the middle of the 20th century, Mullins [18]-[19] had begun to use fracture mechanics theory to study the nucleation and propagation of cracks during rubber fatigue. Under cyclic loading, the stress received at the tip of the internal defect is much greater than the average stress level, and the tip therefore becomes the stress concentration point. When a mechanical defect and a chemical action make a certain defect

reach the damage limitation point, it evolves into a microcrack—fatigue failure begins here [17]. Under cyclic loading, microcracks become an observable macrocrack and continue to expand until the rubber material completely breaks. Therefore, fatigue damage is caused by the gradual destruction of microdefects inside the rubber under cyclic loading [20]-[21].

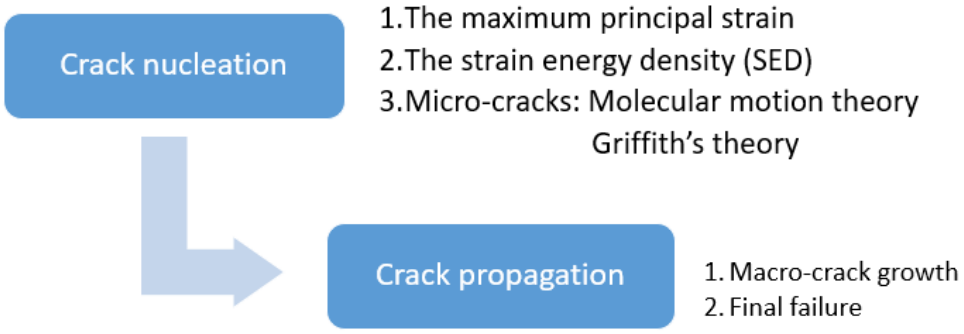

Figure 2.1: Fatigue failure process.

2.3 Factors affecting rubber fatigue

The factors that influence the fatigue performance of natural rubber have been well studied. In order to improve the durability of rubber components, these influencing factors must be qualitatively understood [22]. Only on this basis can fatigue failure be reasonably analyzed.

2.3.1 Frequency

Loading frequency affects the fatigue performance of different types of rubber in different ways. For rubber that produces deformation-induced crystallization, frequency has no obvious influence on fatigue life when the temperature is basically kept constant [23].

For amorphous rubber that does not produce deformation and crystallization, crack propagation is restricted by viscoelasticity, and the loading frequency has a great influence on the fatigue life of the rubber [23].

Under high-deformation and high-frequency loads, the temperature of the specimen increases, and the failure mechanism becomes more complicated [24].

When the internal energy dissipation rate of the rubber is greater than the heat transfer rate with the surrounding medium, the internal temperature begins to rise, causing rapid degradation of the rubber. Some scholars have performed related temperature numerical simulations [25]. The temperature rise of a thicker specimen is more obvious than that in a thinner test piece. In the fatigue test, attention should be paid to measuring and comparing the actual temperature of the rubber, because temperature changes may affect the performance of the material.

For strained crystalline rubber materials such as natural rubber, loading frequencies below 5 Hz will not affect fatigue life [23]. When the loading frequency increases, self-heating will occur. The rate of energy loss inside the rubber is greater than the heat exchange with the environment, causing the internal temperature of the rubber to continue increasing, which causes accompanying effects such as rubber aging and degradation. This in turn affects the anti-fatigue performance of the rubber.

2.3.2 Deformation

Cadwell et al. [26] initially found that increasing the minimum deformation increased the fatigue life of natural rubber. Later, Fielding [27] attempted to verify this result using two new synthetic rubbers, isobutylene isoprene rubber (IIR) and styrene–butadiene rubber (SBR). The findings for IIR agreed with the previous result, but those for SBR did not, indicating that deformation can be extended only by minimizing deformation. Beatty's [28] results for natural rubber compounds also showed that when the minimum deformation increases, the fatigue life can be extended. Lindley [29] initially used the deformation ratio, R (the ratio of the minimum deformation to the maximum deformation, $R = \varepsilon_{min}/\varepsilon_{max}$), to represent the fatigue crack growth rate of natural rubber, as shown in Figure 2.2.

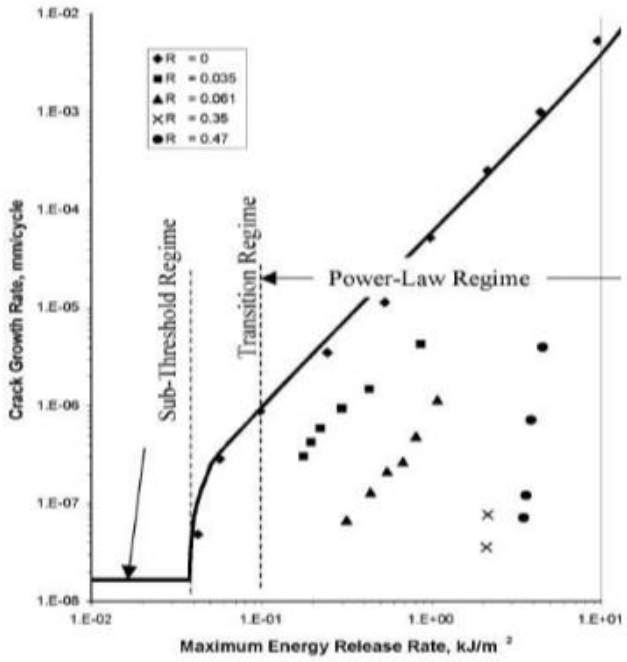

Figure 2.2: Fatigue crack growth curve of unfilled natural rubber when $R > 0$ from [26].

When investigating the effect of a loading condition on a material's fatigue behaviour, researchers typically use the deformation ratio, R, as a parameter. So, the uniaxial test can be divided into three conditions. The first condition is $R < 0$, which means the condition is tension–compression, where the maximum strain is greater than zero and the minimum strain is less than zero. The second condition, when $R = 0$, is the full-relaxation tension test, which means the minimum strain equals zero. The tension–tension condition means $R > 0$. In this condition, the maximum strain and the minimum strain are both more than zero. When researchers investigate the damage mode, they attempt to predict the direction of crack nucleation and crack propagation. Figure 2.3 shows the relationship between the loading condition and the damage mode [30].

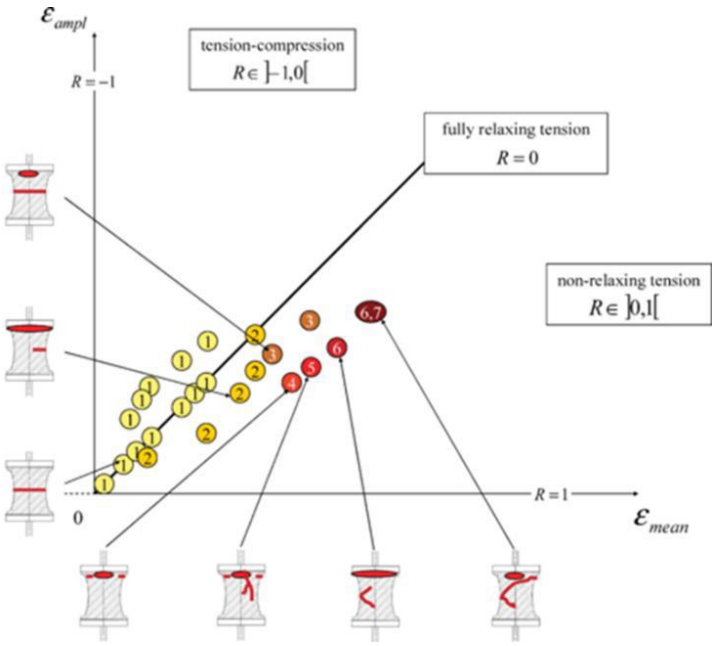

Figure 2.3: The relationship between the loading condition and the damage mode from [30].

2.3.3 Environmental factors

Rubber is used under a wide variety of environmental conditions. Its fatigue performance, which is greatly affected by environmental factors such as oxygen, gas, ozone, chemical media, light, heat, etc., can shorten the fatigue life of rubber. The unsaturated carbon–carbon double bonds in the molecular chain of natural rubber easily interact with oxygen and ozone in the air. Exposure to oxygen causes the degradation and cross-linking of the molecular chain. Ozone can cause degradation only, while a rise in temperature can accelerate the oxidative aging of rubber [31].

High temperature seriously affects the nucleation life and growth rate of rubber fatigue cracks, especially for amorphous rubber. When the test temperature rises from 0 to 100 °C, the fatigue life of SBR decreases 10^4 times, but the fatigue life of natural rubber does not decrease significantly. Adding fillers to raw rubber can improve the sensitivity of the rubber to temperature changes to a certain extent [32]. Shi et al. [33] studied the effect of fatigue temperature on the dynamic bonding properties of steel cord vulcanizates and found that the increase in fatigue temperature caused the appearance of large-scale filler aggregate particles at the interface between rubber and steel cord. Eventually, these particles will lead to interface debonding failure. Factors such as the chemical formula of rubber, vulcanizing agent, and oxidizing agent can change the degree of influence that temperature has on rubber fatigue performance. In addition, an increase in temperature may accelerate the

breaking and cross-linking of molecular chains in natural rubber, change its chemical structure, and affect its fatigue life.

A polymeric substance has three physical states: the glass state, the rubber-elastic state, and the viscosity flow state. In the glass state, the molecular chain of the polymer hardly moves; instead, it becomes very brittle, like glass, and loses its elasticity. When the temperature rises above the glass transition temperature (T_g), a polymer enters the rubber-elastic state. In this state, a polymer shows very good elasticity and the molecular chain segment motion is intensified, but there is no slip between molecular chains. After a force is applied, a rubber part subjected to a large deformation can returned to its initial position. When the temperature is over the viscosity flow temperature (T_f), the polymer begins to enter the viscosity flow state because of the overall movement of the molecular chain. In this state, the melting of the polymer can cause macroscopic flow under the action of a small external force. For natural rubber, $T_g \approx -70$ ℃ and $T_f \approx 130$ ℃. Therefore, natural rubber products usually work in this temperature range.

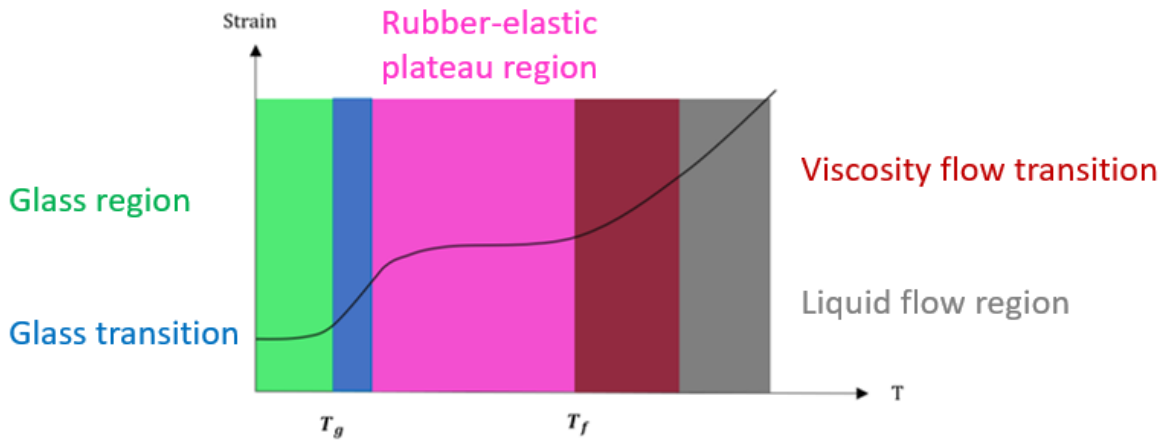

Figure 2.4: The relationship between three states of natural rubber and temperature.

Since the self-heating of rubber affects its aging and degradation, the effect of the working environment temperature on the fatigue behaviour of natural rubber products cannot be ignored. Between -70 and 130 °C, natural rubber shows very good elasticity. Different types of rubber have different degrees of sensitivity to temperature. Compared with natural rubber, SBR is more sensitive to temperature. When the temperature increases from 0 to 100°C, the fatigue life of SBR is reduced by 10^4, times while that of natural rubber drops by only by 4 times [34].

The elongation at break and the fatigue life of natural rubber decreases when the aging temperature and aging time increase [35]-[36]. In addition, the occurrence of heat aging is often accompanied by oxidative aging, which makes the rubber surface hard. Therefore, under cyclic loading conditions, cracks are easily formed and lead to failure in a short time [37]. With the increase of heat aging temperature, the hardness of rubber will also increase,

but the tensile strength and elongation will decrease [38]. Since Charrier et. al [39] focused on the application of rubber materials in the automotive industry, they chose a temperature range of 40 to 120 ℃ for the aging test. They observed that the thermal-oxidation process was evident on the failure surface.

The influence of oxidative aging on the mechanical properties of rubber such as fatigue and fracture are irreversible. Usually, aging causes rubber embrittlement, promotes fatigue crack growth, reduces the critical value of fracture energy, and shortens fatigue life. Studies have shown that for elastic bodies that are more sensitive to deformation, aging affects the slope and intercept of the crack nucleation power function. Blackman et al. [40] studied the influence of various stages of aging on the fatigue life of natural rubber. When the oxygen content reached 1% of its own mass, the fatigue life was reduced by half. The influence of aging on the fatigue properties of rubber also greatly depends on the rubber formulation and processing technology.

In a recent study, Gac et al. [41] conducted uniaxial fatigue tests and crack growth tests on natural rubber. They also evaluated the effect of air and seawater on the fatigue performance of natural rubber under the same R value. They found that under high force, the fatigue life of rubber in seawater is longer than that in air. Because the heat generated in the fatigue process of the specimen is more easily conducted in seawater, the high

temperature of the specimen in the air destroys the stress-induced crystallization that restricts crack propagation, thus accelerating the oxidation of the rubber molecular chain.

Chapter 3: Experimental Setup

3.1 Test specimens

While most recent studies of rubber fatigue have used flat, dumbbell-shaped rubber specimens, dumbbell volumetric samples are generally preferred because they are more representative of rubber parts [42]. It is easier to explore crack growth in the cross-section of a dumbbell volumetric specimen, and this configuration is well adapted to fatigue, since no bucking is induced under compression [42]. Therefore, to investigate the fatigue behaviour of natural rubber, the test specimens needed to have a dumbbell volumetric shape.

All samples were purchased from the Elesa USA Corporation. The natural rubber material used had a hardness of 55 Shore A and a formulation typical of vibration isolators. Figure 3.1 shows the configuration of the samples.

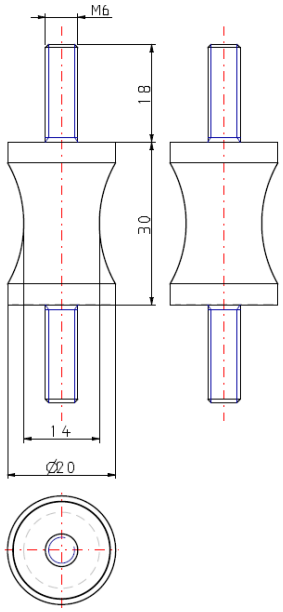

Figure 3.1: Configuration of the samples (dimension in mm).

3.2 Testing equipment

Uniaxial tensile testing was carried out using the ElectroPuls E3000 Linear-Torsion All-Electric Dynamic Test Instrument (Instron Company, Norwood, Massachusetts, USA), a state-of-the-art, all-electric test instrument designed for dynamic and static testing of a wide range of materials and components (Figure 3.2).

Figure 3.2: ElectroPuls E3000 Linear-Torsion All-Electric Dynamic Test Instrument.

An environmental chamber (Instron Company; Figure 3.3) was used to adjust the temperature of the sample from ambient temperature to 350 ℃ during the test.

Figure 3.3: Environmental chamber.

During the fatigue test, the temperature change of the rubber sample was measured by an FLIR A6700 MWIR thermal camera (FLIR Systems, Wilsonville, Oregon, USA; Figure 3.4). Designed for electronics inspections, manufacturing monitoring, scientific research, and nondestructive testing, the camera is ideal for high-speed thermal events and fast-moving targets.

Figure 3.4: FLIR A6700 MWIR thermal camera.

According to the testing standard ASTM D572-04, rubber samples should be exposed to certain temperatures in an aging oven (Figure 3.5) for several days (ProJet Finisher Oven). This part of the experiment is described in section 3.3.5.a on thermal aging.

Figure 3.5: Aging chamber.

3.3 Specimen test methods and procedures

In the aerospace, automotive, construction, and other industries, natural rubber is often used as a raw material in antivibration products to reduce or eliminate the transmission of mechanical vibration, thus enabling shock absorption, noise reduction, and impact damage reduction. Natural rubber antivibration products are usually served in the state of a cyclic alternating spiral, which is easy to fatigue and lose under the action of cyclic stress.

Among the complex fatigue forms, tensile fatigue is the simplest uniaxial fatigue damage method. It is the basis for studying the complex fatigue characteristics of rubber and is of great significance in predicting the service life of actual components.

Our primary research objective was to investigate a testing protocol and compare it with ASTM D4482-11 standard. Since the deformation and frequency need to be examined in this experiment, our research attention is also dedicated to the internal heat that it is unavoidable. Moreover, our experimental system allows us to monitor the applied load during the entire test and record load history. Another obvious difference between this experiment and ASTM D4482-11 is the shape of the sample. The ASTM standard uses dumbbell-shaped rubber sheets, but our experiment uses dumbbell-shaped rubber samples in order to minimize the sample edges on fatigue sample performance. Therefore, the crack propagation process can be understood more accurately

A reference experiment is needed to study the influence of various factors on the fatigue life of natural rubber. All experimental data were compared with this reference group. The uniaxial tensile test was strain controlled, with the maximum strain of 50% set at a frequency of 10 Hz.

All tests were performed at room temperature (23 °C). In this study, the criterion of fatigue failure was the complete fracture of the rubber sample.

3.3.1 Factor of deformation

Based on the reference experiment, the factor that needs to be changed is strain level. In this uniaxial tensile test, the deformation should be 25%, 50%, and 75% strain at 10 Hz. All tests were performed at room temperature.

3.3.2 Factor of frequency

When studying the influence of frequency on the fatigue life of natural rubber, the deformation is 50% strain level, but the frequencies of the loaded sine curve are 1, 2.5, 5, 7.5, and 10 Hz. All tests were performed at room temperature.

3.3.3 Temperature conditions

Compared with the reference experiment, the temperatures in this group of experiments were 50 °C and 80 °C. This temperature range was chosen because natural rubber is in a

rubber-elastic state between 20 °C and 100 °C, which is also the temperature range where rubber products often work.

3.3.4 Factor of size

Samples of different shapes are used when studying the fatigue characteristics of rubber. The most common include flat, dumbbell-shaped rubber sheets, diabolo-shaped rubber bodies, and cylindrical rubber blocks. This experiment used samples of the same shape but different sizes to compare fatigue failure characteristics. The specific experiment requirements were the same as those of the reference experiment.

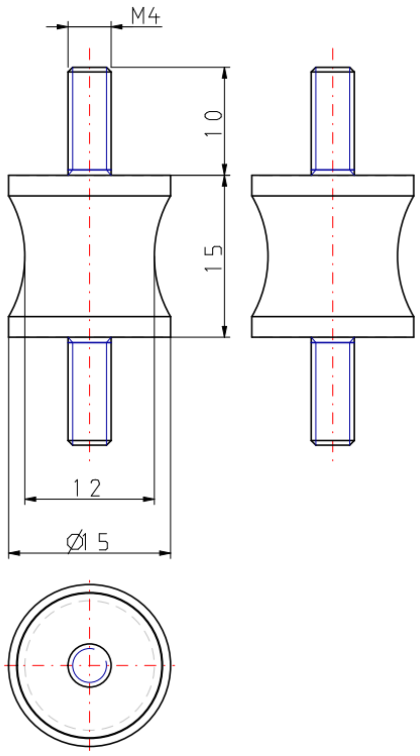

Figure 3.6: Configuration of small samples (dimension in mm).

3.3.5 Aging conditions

3.3.5.a Thermal aging effect

According to ASTM D572-04, rubber samples should be exposed to 120 °C for 2, 4, 8, and 16 days in order to evaluate the impact of thermal aging on the properties of the material. After the thermal aging treatment, the samples need to be cooled to room temperature on a flat surface and allowed to rest for at least 16 h but no more than 96 h before performing the uniaxial tensile test.

3.3.5.a Liquid aging effect

According to ASTM D571, the samples were immersed in reference oil IRM 902 for 70 and 166 h under dark conditions (Figure 3.7). After the sample was removed from the oil, the same experimental steps were performed as those done in the reference experiment.

Figure 3.7: Reference oil IRM 902.

3.4 Test plan

Table 3.1 shows the experimental plan for the entire study.

Table 3.1 Test plan.

Factors	Testing Condition	Number of Tested Sample
Deformation	25%, 23 °C, 10Hz	4
	50%, 23 °C, 10Hz	6
	75%, 23 °C, 10Hz	6
Frequency	50%, 23 °C, 1Hz	6
	50%, 23 °C, 2.5Hz	6
	50%, 23 °C, 5Hz	6
	50%, 23 °C, 7.5Hz	6
	50%, 23 °C, 10Hz	6
Temperature	50%, 10Hz, 50℃	6
	50%, 10Hz, 80℃	6
Size	Small size sample, 50%, 23 °C, 10Hz	3
Thermal Aging	50%, 23 °C, 10Hz, 120℃ 2days	4
	50%, 23 °C, 10Hz, 120℃ 4days	4
	50%, 23 °C, 10Hz, 120℃ 8days	2
	50%, 23 °C, 10Hz, 120℃ 16days	4
Liquid Aging	50%, 23 °C, 10Hz, 70h	6
	50%, 23 °C, 10Hz, 166h	6

Chapter 4: Results and Discussion

This chapter is divided into two parts. The first part shows how the fatigue life of rubber changes under the influence of different factors. The second part is to observe the fracture cross section of the sample to understand the crack propagation mode and direction from a macro perspective.

4.1 Fatigue life analysis

This part mainly analyzes the relationship between fatigue life and various influencing factors. It also uses the fatigue life curve to characterize the entire process of the fatigue failure of rubber samples. The reference experiment data are presented as an example.

Under the requirements of the reference experiment, a total of nine experiments were carried out. The number of cycles for each experiment is shown in Table 4.1.

Table 4.1: Reference experiment data.

Sample No.	No. of cycles
1	106 694
2	99 952
3	92 450
4	107 295
5	100 000
6	115 542

According to these six sets of data, the average fatigue life cycle is 103 655, with a standard deviation of 7262. Therefore, sample 1 was chosen because it was the sample with a fatigue life cycle closest to the average reference value.

Figure 4.1 shows the relationship between load and fatigue life cycles and the entire fatigue failure process of a rubber sample. It is divided into three parts from left to right. The first part is the beginning of the experiment. Because the stress changed sharply, the phenomenon of stress softening appeared. Then, in the second part, the curve enters a plateau. The stress changed slowly, and microcracks were generated on the surface of or inside the rubber material, a phenomenon referred to as crack nucleation. In the last part, the curve had a significant turning point. Usually at this time, visible cracks of 2 to 3 mm on the surface of the rubber sample can be observed. When macrocracks appear, the rate of crack propagation is very fast, and then the sample will be completely broken.

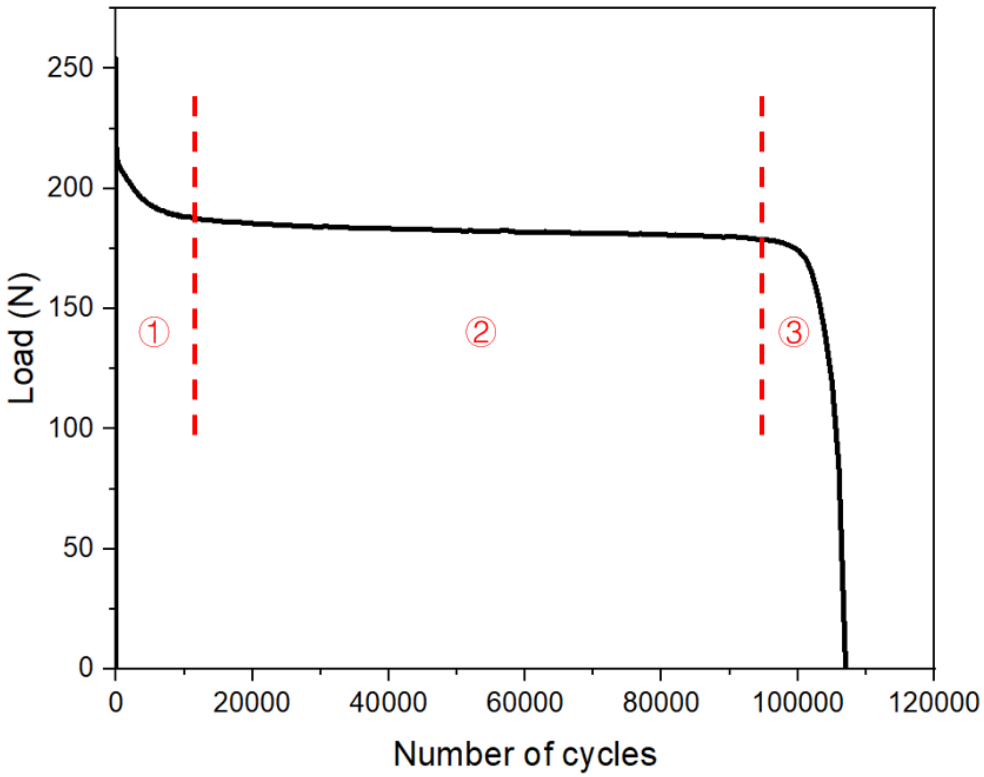

Figure 4.1: The relationship between fatigue life and load of reference experiment.

4.1.1 Deformation effect

Figure 4.2 shows the life cycles of natural rubber samples under different levels of strain. When deformation is 25%, the fatigue life is about 1 million cycles, which is 10 times the fatigue life at a deformation of 50%. When deformation is 50%, the fatigue life is about 100 000 cycles, which is 6 times the fatigue life at a deformation of 75%.

The amount of deformation has a significant impact on the fatigue life of rubber. The greater the deformation, the greater the force that the rubber mesh chain bears, resulting in

severe stress concentration and accelerating the fracture of the chain with lower bonding strength.

During testing, the natural rubber sample is stretched by a cyclic external force and generates heat owing to the internal friction of the molecular chain. This heat also has an impact on the fatigue life of rubber.

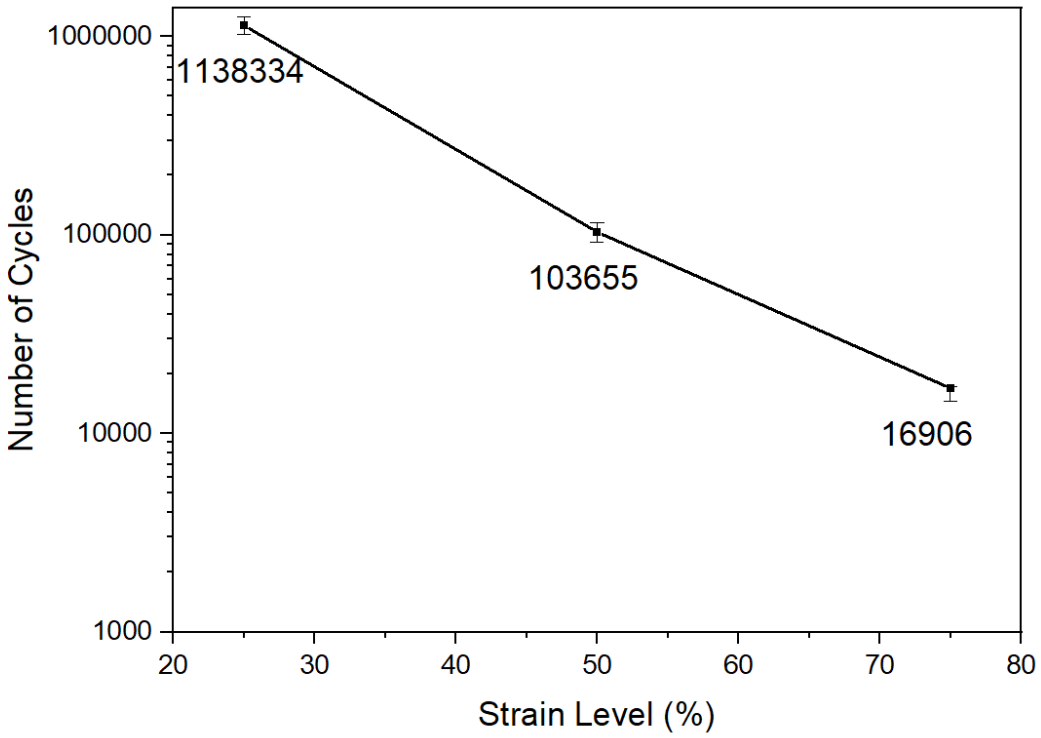

Figure 4.2: Fatigue life of natural rubber samples at different deformations.

Table 4.2 shows that at a 25% strain level, the surface temperature of the rubber sample was 55 °C. When the deformation was 50%, the surface temperature of the sample was 78 °C. The highest surface temperature of a sample was 106 °C, at a deformation of 75%.

The temperature difference in the heat generated by these three levels of strain was about 30 °C.

Table 4.2: The surface temperature of the sample during the experiment.

	Deformation		
	25%	50%	75%
Temperature of sample (°C)	55	78	106

According to Figure 4.3, as the amount of deformation decreases, the tensile force on the rubber samples decreases, but both deformation and the tensile force have similar fatigue curves and characteristics.

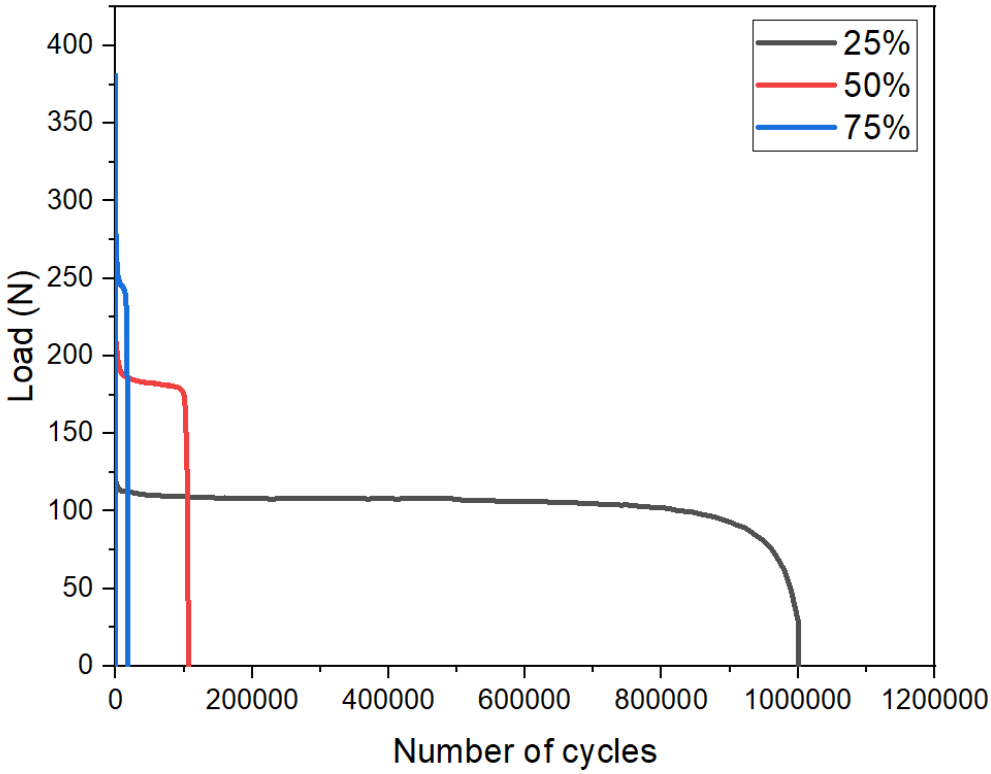

Figure 4.3: The relationship between fatigue life and load of different deformations.

4.1.2 Frequency effect

The fatigue life cycles of the samples varied with frequency (Figure 4.4). When the frequency was increased from 1 to 5 Hz, the fatigue life also increased. When the frequency continued to increase to 10 Hz, however, the fatigue life decreased.

Under low-frequency conditions, the molecular chain breakage caused by mechanical fatigue damage plays a decisive role; under high-frequency conditions, owing to the large increase in the amount of heat generated, the main cause of damage is not mechanical fatigue, but rather thermal degradation caused by the high temperature. Chemical changes play an important role in the destruction of rubber [38]. Therefore, in the next step, a thermal camera was used to detect the temperature of the sample during testing.

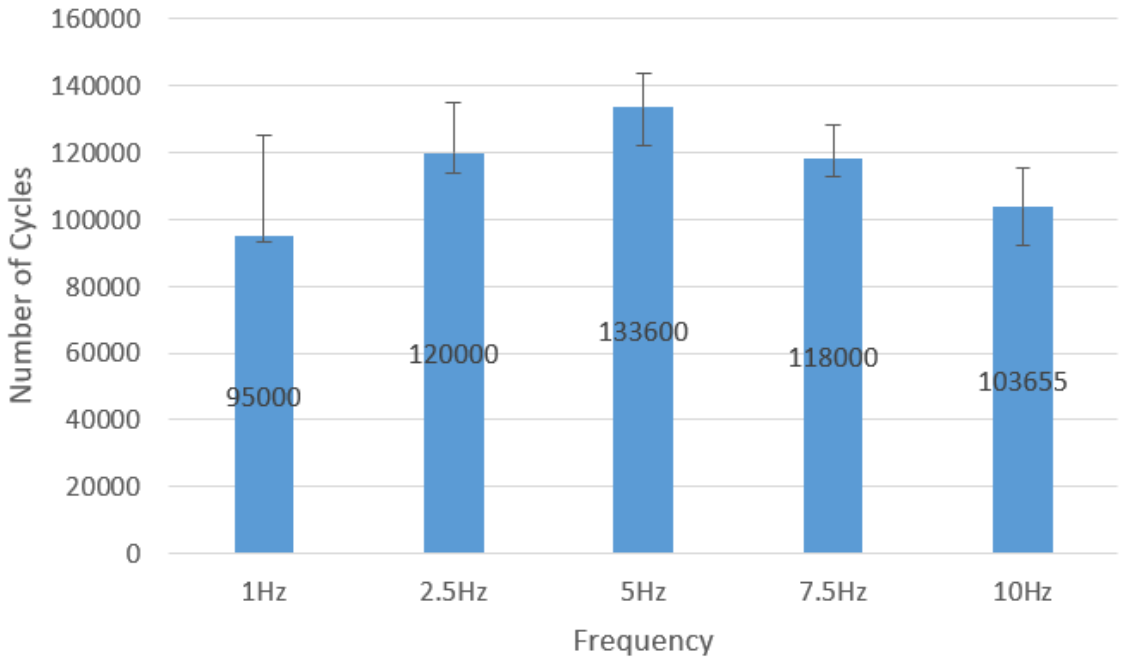

Figure 4.4: Fatigue life of natural rubber samples at different frequencies.

Figure 4.5 shows the temperature at the centre of the sample measured by a thermal camera. As the frequency increased, the temperature inside the sample also increased. Samples at all frequencies reached a relatively stable temperature within a similar time frame (~750 s), and the temperature no longer increased. The higher the frequency, the faster the heating rate.

At a frequency of 1 Hz, the surface temperature of the rubber product stabilized at ~32 °C. At 2.5 Hz, the temperature stabilized at about 39 °C. At 5 Hz, the surface temperature of the sample was 54 °C. The surface temperature of the 7.5 Hz sample reached 63 °C. At 10 Hz, the fastest frequency, the surface temperature of the sample was also at its highest, reaching 78 °C.

The higher the loading frequency, the faster the internal structure of rubber changes over time. As the movement of the rubber macromolecular chains intensifies, there is increased interaction between molecular chains and additives.

The large amount of heat generated by friction between molecular chains cannot be exchanged with the external environment in time, so the surface temperature of the sample is increased, thereby accelerating the initiation and propagation of cracks, and reducing the fatigue life of the rubber.

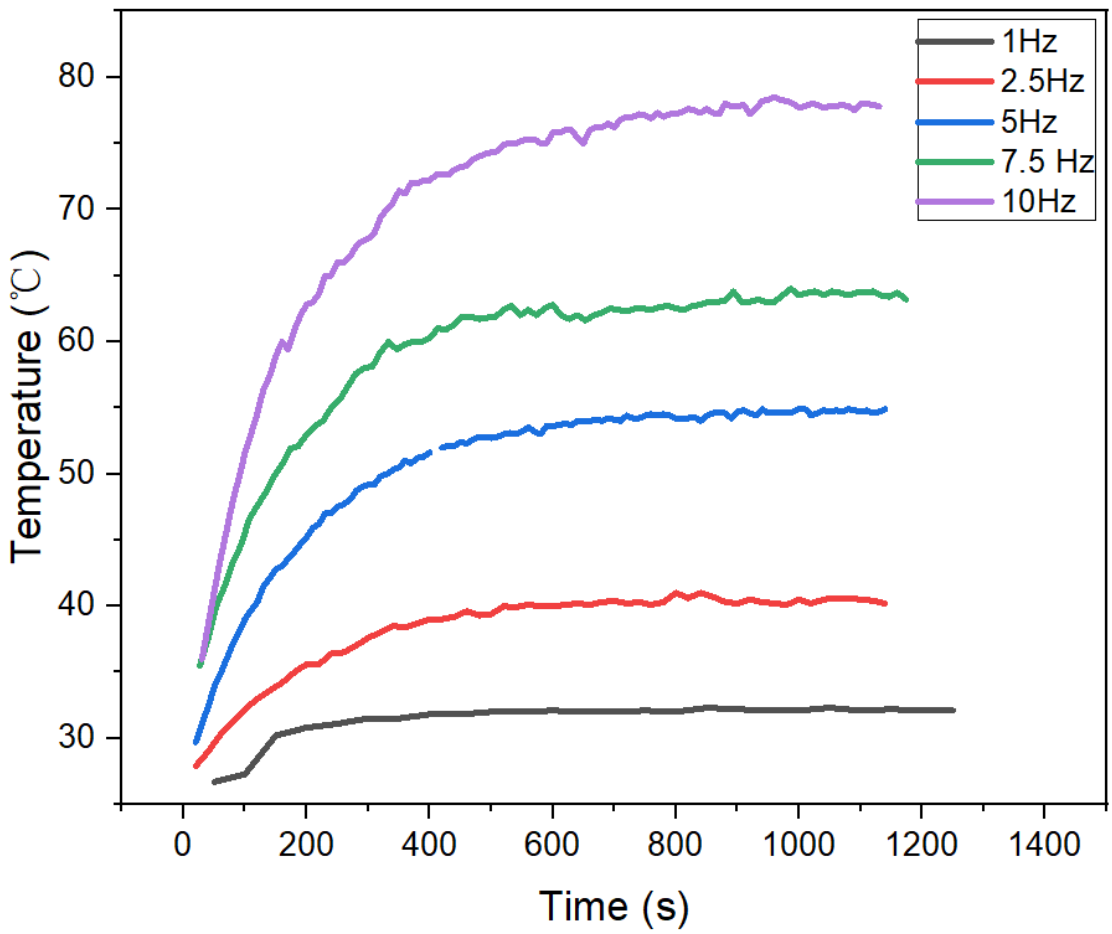

Figure 4.5: Samples surface temperature at different frequencies.

When the temperature increases appropriately, such as to 54 °C, heat increases the mobility of molecules in the rubber. Then the stress relaxation rate can increase, which leads to a decrease in stress concentration. The stress concentration is reduced, thereby reducing the possibility of molecular chain breaking, and the natural rubber samples are difficult to fatigue.

However, as the temperature rises too high, such as to 78 ℃, owing to poor thermal conductivity it is difficult for rubber to dissipate fatigue heat. The further the temperature

rises, the more likely it is to cause thermomechanical damage and increase thermal oxidation to accelerate fatigue. Proper heating can extend the fatigue life of rubber, but the heat generated by too high of a temperature will accelerate the breakage of molecular chains, which accelerates fatigue. Therefore, when conducting temperature experiments, the choice of 50 and 80 °C allows the influence of external temperature on fatigue aging life to be observed.

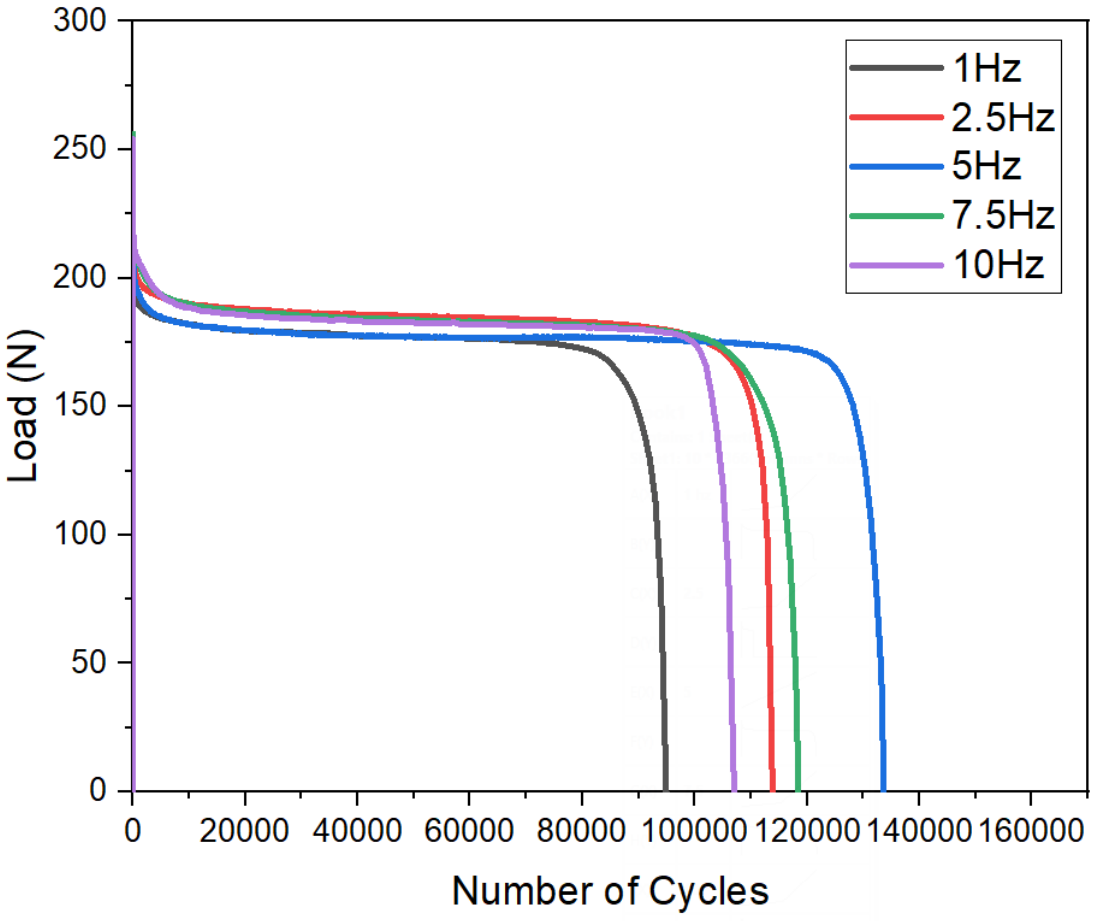

Figure 4.6: The relationship between fatigue life and load of different frequencies.

Figure 4.6 shows the relationship between the force on the sample and the fatigue life at different frequencies. When the tensile test entered a plateau, although the external force experienced by the sample was basically the same under different frequency conditions, the load was about 185 N. However, the time at which macroscopic cracks began to appear on the surface of the sample varied with the frequency. In the last stage, the crack propagation rate was basically the same because the descending curves were almost parallel.

The loading frequency affects the sample temperature during the test. The surface temperature of the sample affects the crack nucleation of natural rubber. When macroscopic cracks appear on the surface, as the cracks increase, the surface temperature has almost no effect on the crack propagation rate.

4.1.3 Temperature effect

Figure 4.7 shows the number of fatigue life cycles under different environmental temperatures. With increasing temperature, the number of fatigue life cycles decreased. When the outside temperature rises, it is difficult to dissipate the heat generated by the rubber sample, which also increases the sample temperature. Therefore, thermal oxidative degradation becomes the main reason for accelerating the fatigue behaviour of natural rubber.

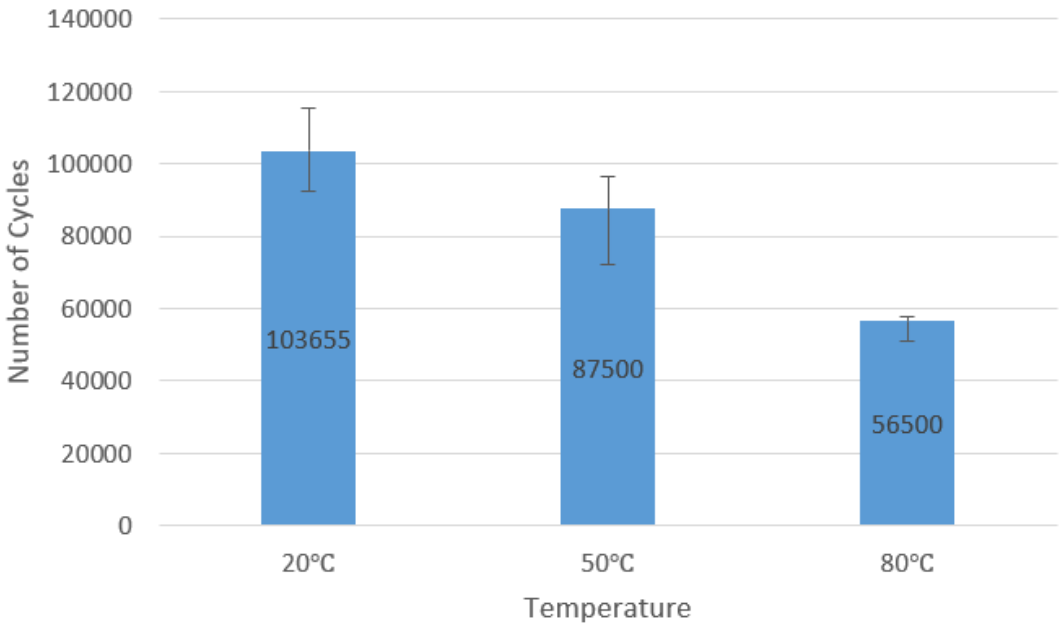

Figure 4.7: Fatigue life of natural rubber samples at different ambient temperatures.

The relationship between load and fatigue life under different temperatures is shown in Figure 4.8. At the beginning of the experiment, owing to the phenomenon of stress softening, the load gradually decreased until it remained basically unchanged. In the stable phase of the experiment, the environmental temperature did not affect the load, which was 185 N. However, the fatigue life of rubber at 80 °C was significantly shortened. When macrocrack appeared, the crack growth rate seemed to be the same.

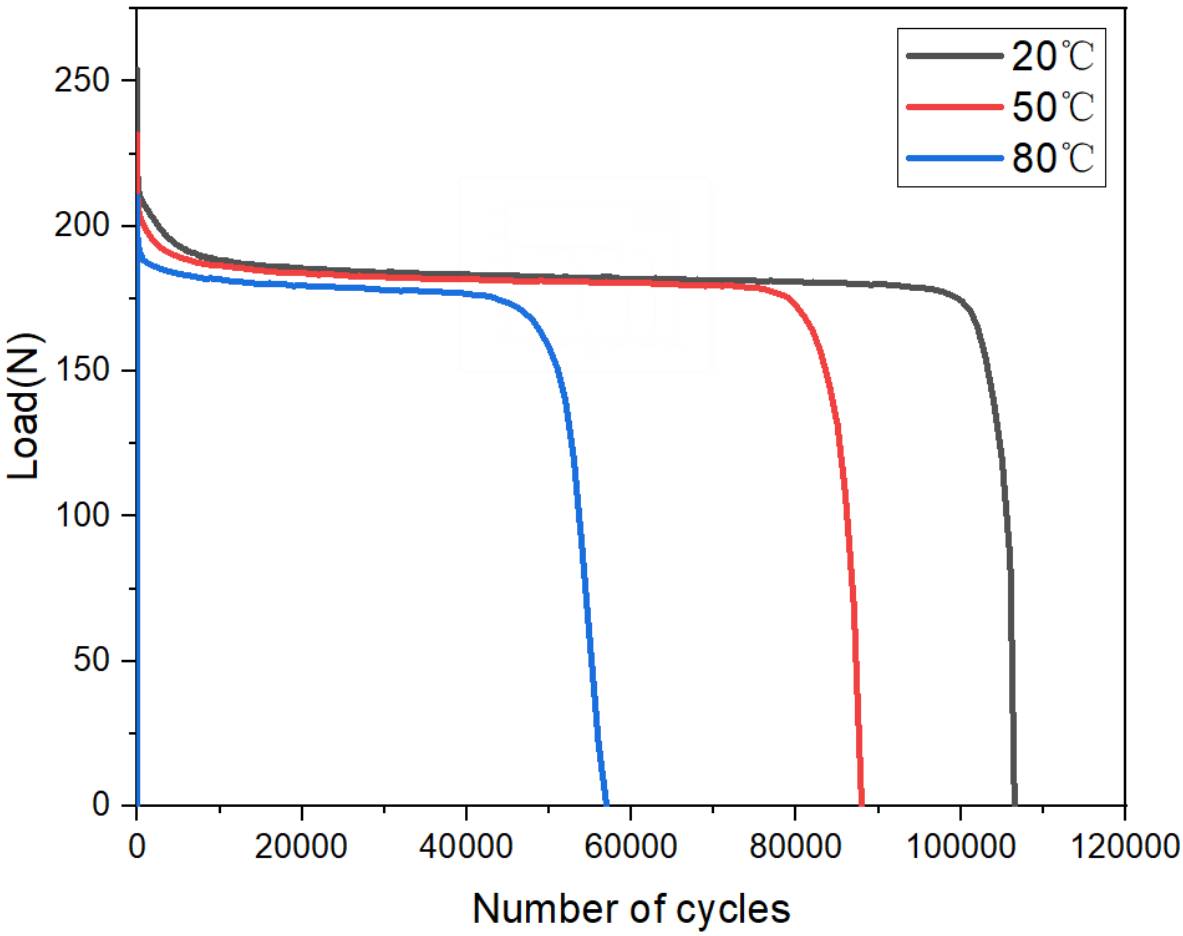

Figure 4.8: The relationship between fatigue life and load of different temperatures.

4.1.4 Size effect

The length of the test sample was half that of the reference sample. The diameter through the test sample centre was 2 mm shorter than that of the reference sample. Under the same experimental conditions, the fatigue life of the small sample was about 70 000 cycles, which is 70% that of the reference sample.

As observed by the thermal camera, the surface temperature of the small sample in the experiment was about 61 °C, which was 17 °C lower than the centre temperature of the reference sample.

According to Figure 4.9, the fatigue characteristics of the two samples are the same, but after entering the plateau, the load of the small sample is smaller, about 150 N.

After entering the crack growth stage, the curve of the small sample is slightly flat when it drops. In other words, the crack propagation rate should be slower.

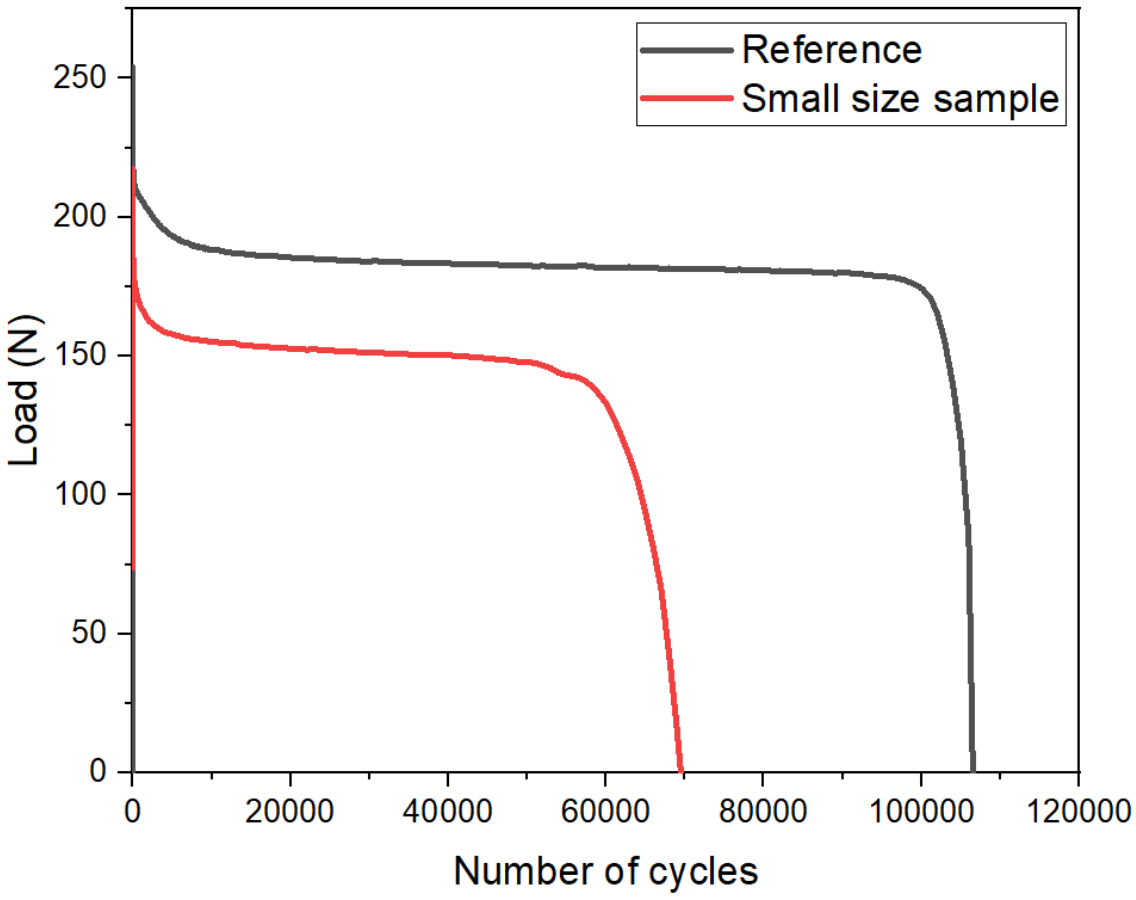

Figure 4.9: The relationship between fatigue life cycles and load of different sizes.

4.1.5 Aging effect

4.1.5.a Thermal aging

Samples were placed in an aging chamber and aged at 120 °C for 2, 4, 8, and 16 days. Then, the same tests were performed with same requirements as those used in the reference experiment.

As Figure 4.1 shows, when the aging time is 2 days, the fatigue life is about 70 000 cycles. The fatigue life is greatly reduced to 13 874 cycles when the aging time is 4 days. When the aging time is 8 and 16 days, the fatigue life of the rubber samples is only 4700 and 3598 cycles, respectively, which is slightly lower than the fatigue life of the samples aged for 4 days. However, the fatigue life of the unaged sample was about 20 times longer than that of the samples aged the longest.

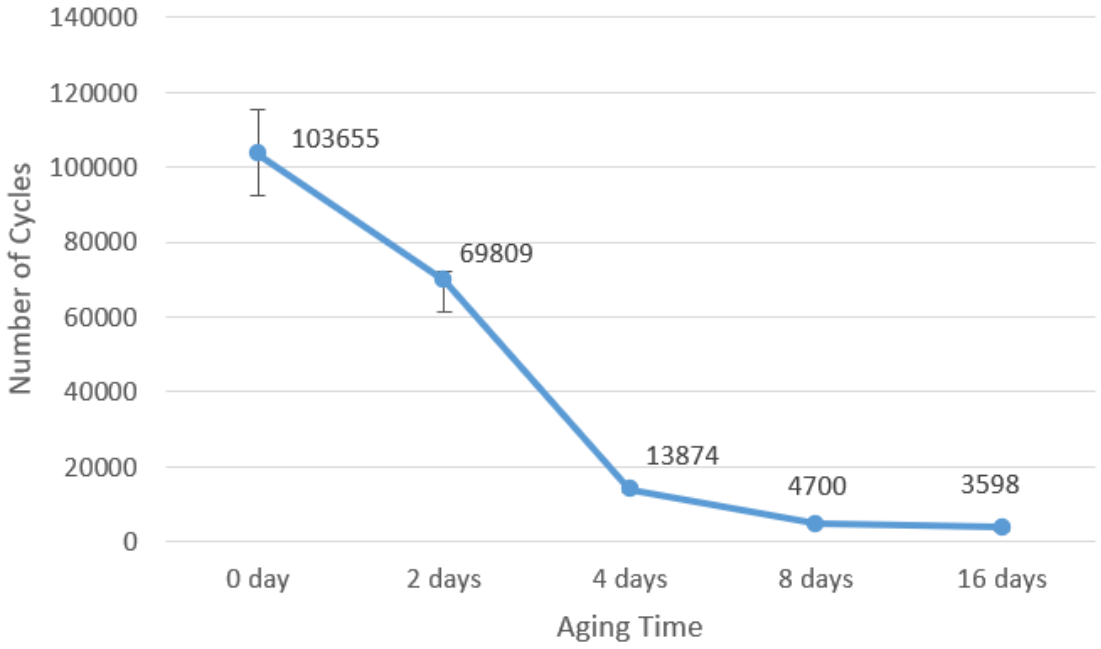

Figure 4.10: Fatigue life of natural rubber samples at different aging times.

The relationship between aging and load is shown in Figure 4.11. Compared with the unaged rubber sample, the sample aged for 2 days had the same tensile strength in the plateau period, but the fatigue life was short. The curve of the sample aged for 4 days basically conformed to the fatigue characteristic curve of the unaged sample, but its tensile strength is reduced, with a load of about 150 N, and the sample failed quickly. The curves of the samples aged for 8 and 16 days are completely different from those of the unaged samples, which shows that heat aging greatly changes the physical properties of rubber. Figure 4.11 clearly shows the fatigue characteristics of the samples.

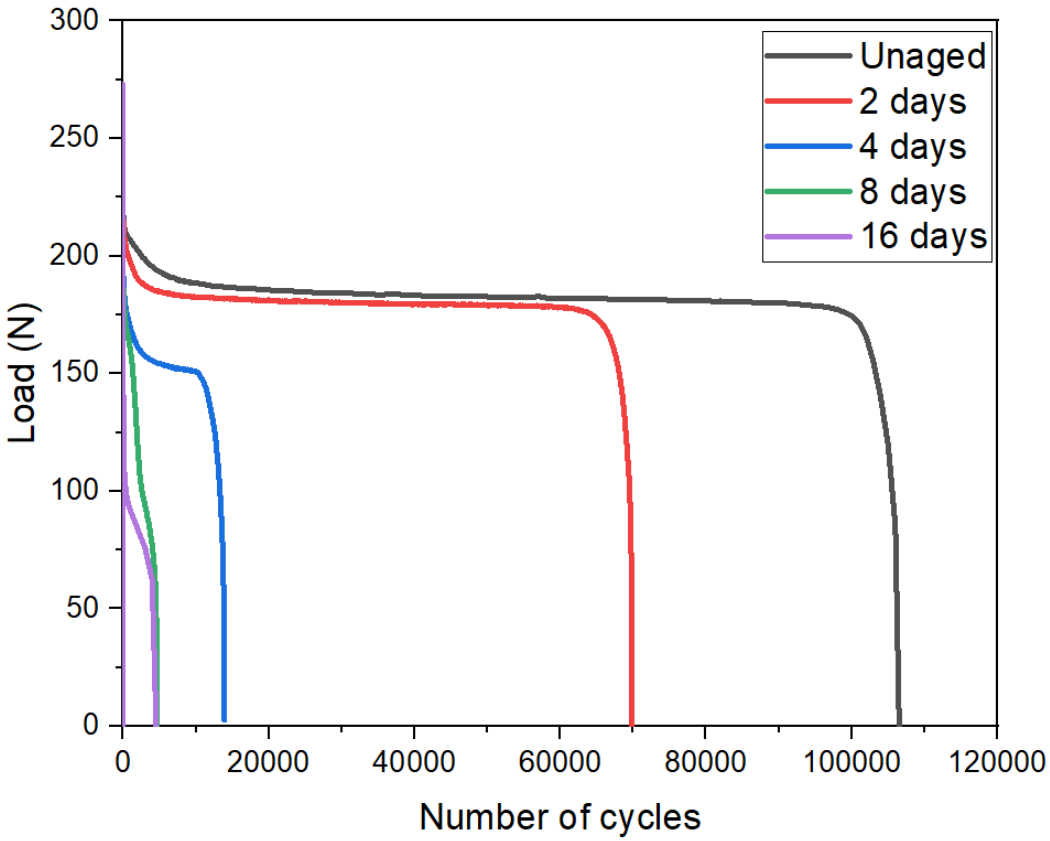

Figure 4.11: The relationship between fatigue life and load of different aging times.

According to the broken blue line, the fatigue failure process can be divided into two stages, but the failure process of samples aged for 8 and 16 days was not the same.

For samples aged 8 days, there was also a stress softening phenomenon at the beginning of the experiment, so the load gradually decreased. However, the curve did not enter a plateau afterwards but continued to gradually decline. Until entering the second stage, the curve showed a significant turning point, and then the sample failed.

For the sample aged for 16 days, the load drop at the beginning of the experiment was not the result of stress softening. Instead, the rubber sample lost its elasticity and became brittle

because of a long aging period. When the sample was stretched under a huge load, multiple cracks immediately appeared on the surface of the sample, a phenomenon referred to as brittle fracture. After that, the load on the sample dropped almost linearly. Since cracks had appeared on the surface of the sample, this part of the curve represents the crack propagation area. When entering the second part of the curve, there was a clear turning point. At this stage, because the previous stress was concentrated on a certain crack, the plane where the crack was located eventually developed into a fracture section, and the sample failed.

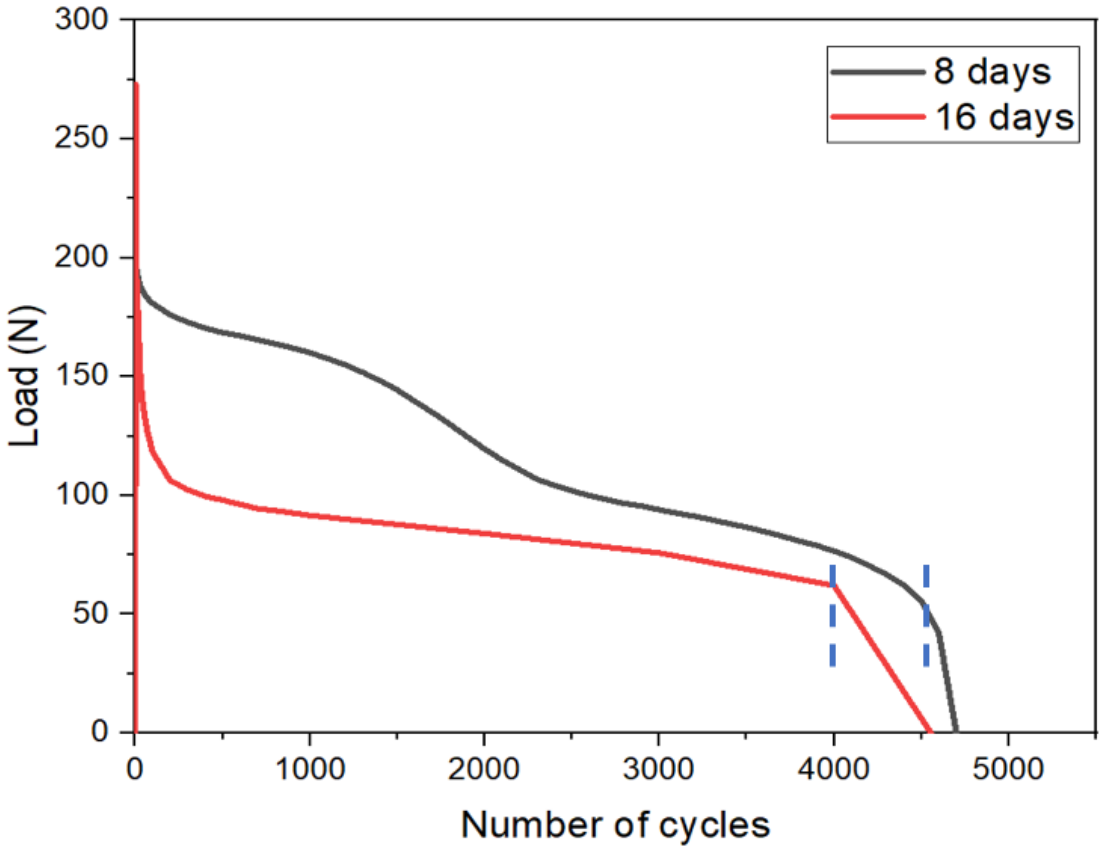

Figure 4.12: The relationship between fatigue life and load of 8 and 16 days aging.

During the high-temperature aging process, the breakage of the molecular chains in the natural rubber led to a change in the chemical and physical properties of the sample. As the aging time increased, the internal molecular chain breakage also increased. The rubber sample became brittle, and the elasticity of the rubber sample decreased. Therefore, the fatigue life was also greatly reduced, and different fatigue failure processes became evident.

4.1.5.b Liquid aging

Figure 4.13 shows that the curve of the sample with an aging time of 70 h almost coincides with the curve of the unaged sample. The tensile strength of the sample did not change either. The fatigue life of the sample with an aging time of 166 h was slightly longer than that of the unaged sample by 10 000 cycles. During this time, liquid aging had almost no effect on the fatigue resistance of the rubber samples.

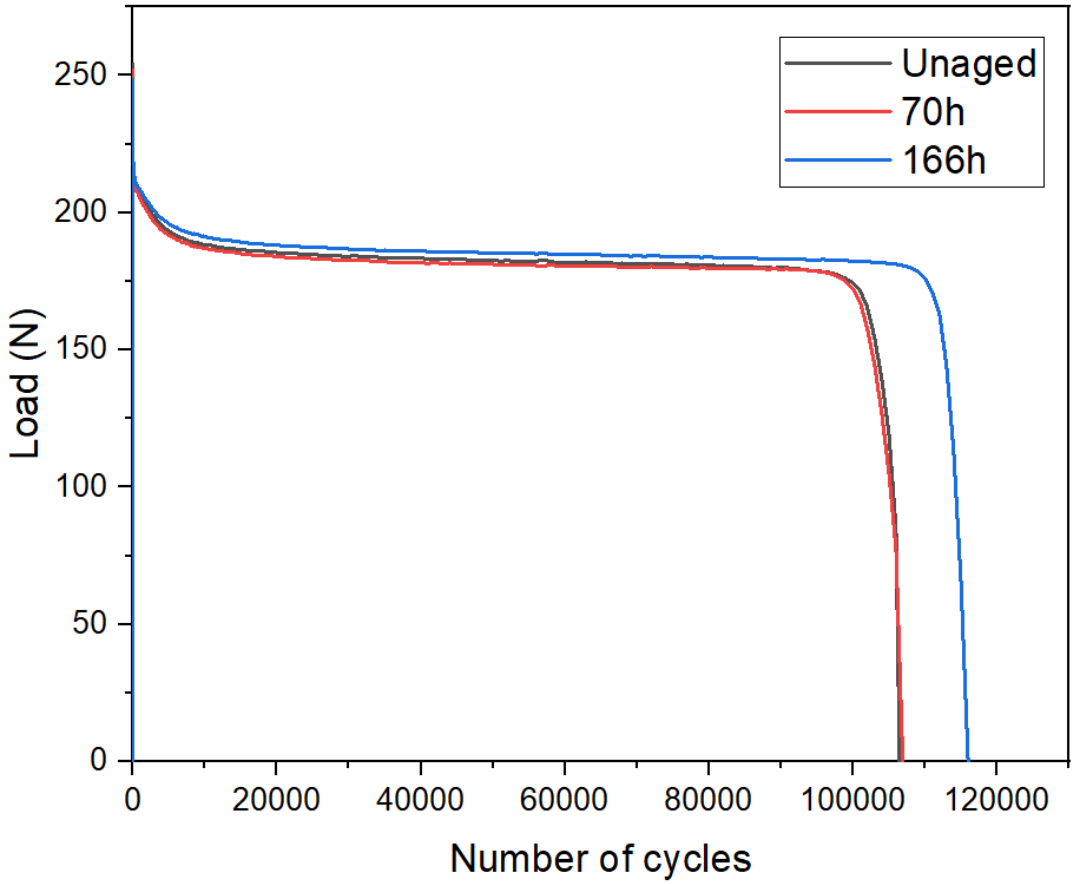

Figure 4.13: The relationship between fatigue life and load of different liquid aging times.

4.2 Fracture characteristics

This section includes an analysis of the fracture cross-section of the rubber sample. The similarities and differences of fracture modes were investigated under the influence of various external factors from a macro perspective. Figure 4.14 shows the fracture cross-section of the reference experimental sample.

(a)

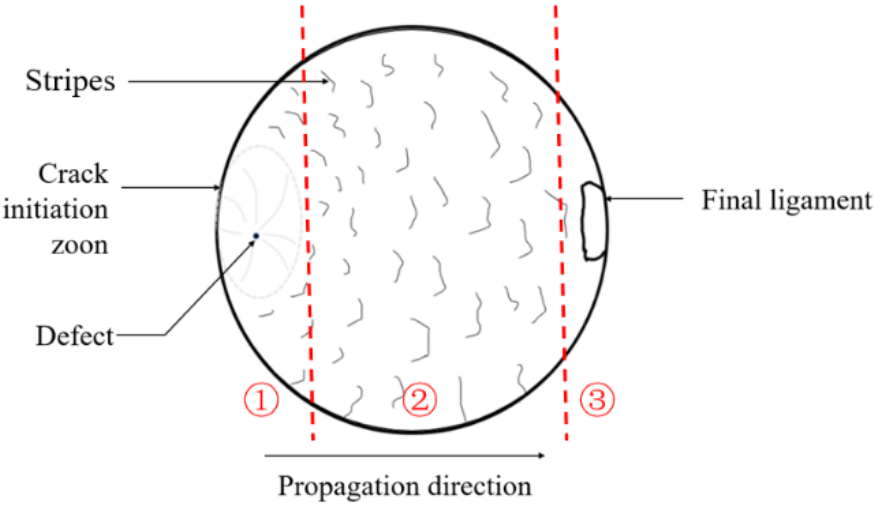

(b)

Figure 4.14: (a) Reference experimental sample fracture and (b) interface and schematic diagram.

According to experimental observations, the direction of crack propagation was from left to right. The fracture section can be divided into three parts: the crack initiation zone, the crack growth zone, and the final ligament zone. Part 1 is the crack initiation zone, which is

always located close to the surface of a sample. The reason why the initial crack always appears on or near the surface of a test coupon is because during the uniaxial tension test, the total length of the coupon increases and the cross-sectional area becomes smaller. However, the deformation of the outer surface is the largest, and the molecular chain moves the most violently, and hence the surface of the test coupon easily becomes the region of stress concentration. The direction of crack growth is usually perpendicular to the direction of the load. This zone is identified by the orientation of the stripes on the fracture surface.

Part 2 is the zone corresponding to crack propagation through the bulk of the sample. In Figure 4.14, it is indicated by a pattern of stripes. This area represents a period when the crack propagation rate is relatively stable, and crack propagation is also stable. As the crack grows, the surface becomes rough.

Part 3 corresponds to the final fracture surface and is very smooth. A brittle fracture occurred in this part of the sample, and a small piece of rubber eventually broke away from the test coupon, causing the sample to completely fracture and fail.

4.2.1 Deformation effect

Figure 4.15 shows the fracture interface morphology of the rubber sample under different levels of strain. The fracture surface of the sample with a deformation of 25% is flat and has only a few fine lines. Compared with the reference experimental sample, there is no

third-stage brittle fracture region. The entire crack propagation process is smooth and uniform. The fracture surface of the sample with a strain level of 75% is rougher. The direction of crack propagation is not perpendicular to the direction of the force but inclined. Compared with the reference experimental sample, the brittle fracture region in the last stage is larger.

As the amount of deformation increased, the fracture surface of the sample became increasingly rougher, and the final brittle fracture area increased.

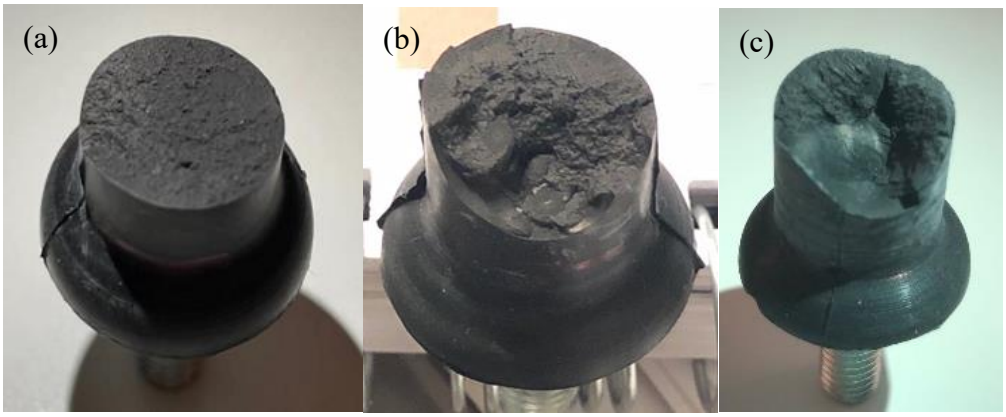

Figure 4.15: Fracture surface of sample at (a) 25% (a), (b) 50%, and (c) 75% strain level.

4.2.2 Frequency effect

Figure 4.16 shows the macroscopic morphology of the fractured surface of rubber samples at different frequencies. The fracture planes of these samples were relatively flat overall. For the first three types of samples, their fracture process shows only the first two stages; because there was no third brittle fracture stage, their fracture surface shows stripes only.

As the frequency increased, the fracture surface became increasingly rougher. When the frequency increased to 7.5 Hz, a third zone appeared on the fracture surface. This also provides evidence that the fatigue life of the sample was reduced as a result of the appearance of brittle fracture, because brittle fracture occurs in an instant. The larger the brittle fracture area of the third stage, the shorter the fatigue life of the sample.

In conclusion, as the frequency increased, the fringes on the surface of the sample in the crack extension zone became rougher. When the frequency exceeded 5 Hz, a third brittle fracture zone appeared on the fracture surface, which is also the reason for the shorter fatigue life of the rubber sample.

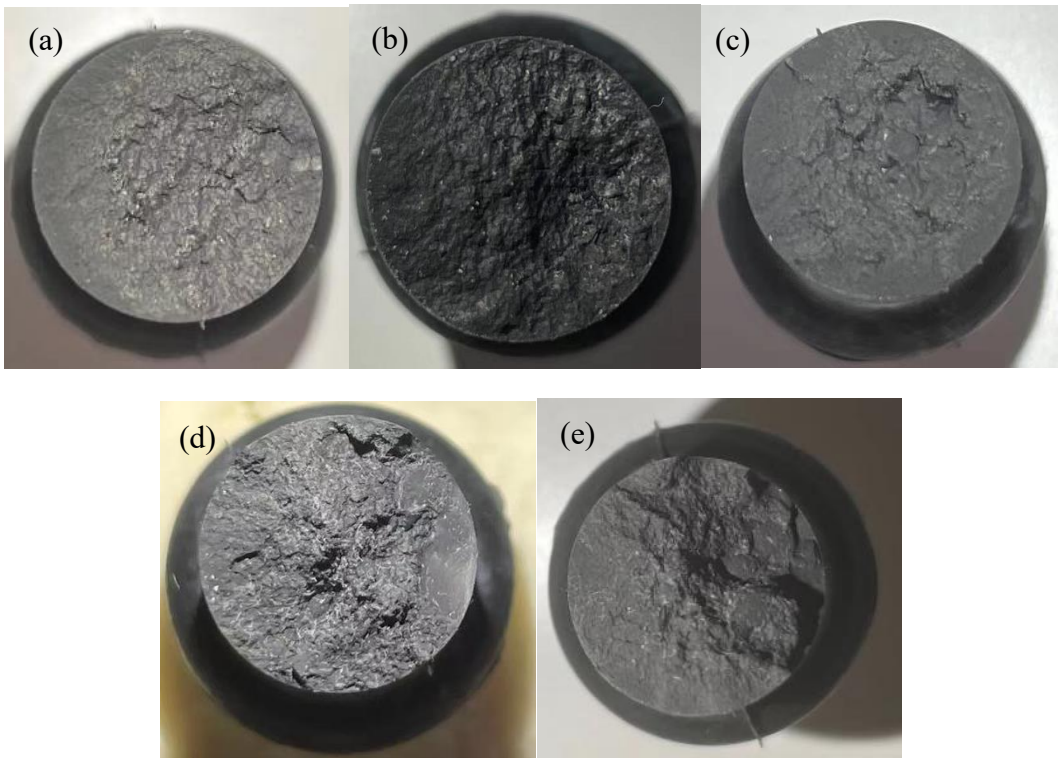

Figure 4.16: Fracture surface of sample at (a) 1Hz, (b) 2.5Hz, (c) 5Hz, (d) 7.5Hz, and (e) 10Hz.

4.2.3 Temperature effect

From the top view (Figure 4.17), the crack propagation conditions reflected by the fracture interface of the rubber samples at different temperatures were basically the same, and they all transitioned through the three stages of crack propagation. However, from the side view shown in Figure 4.18, as the temperature increased, the overall fracture section of the sample became increasingly uneven. In other words, the direction of crack propagation was not perpendicular to the direction of force but inclined upward or downward.

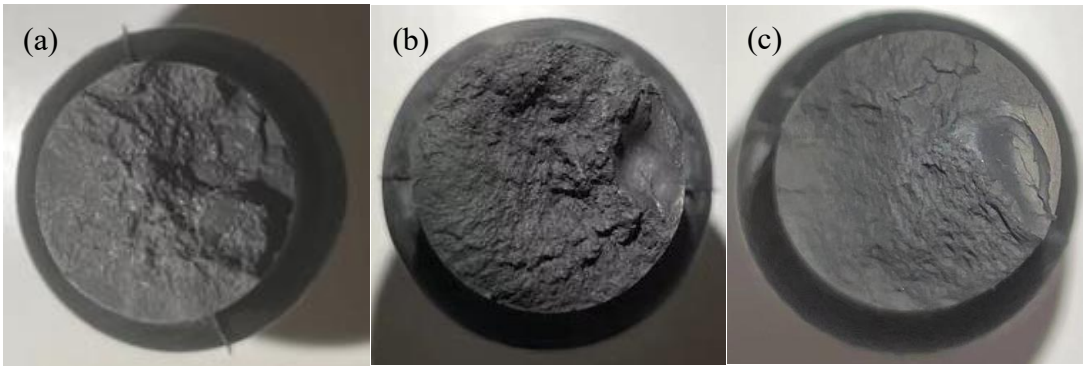

Figure 4.17: Top view of the fracture surface of a sample at (a) 20 ℃, (b) 50 ℃, and (c) 80 ℃.

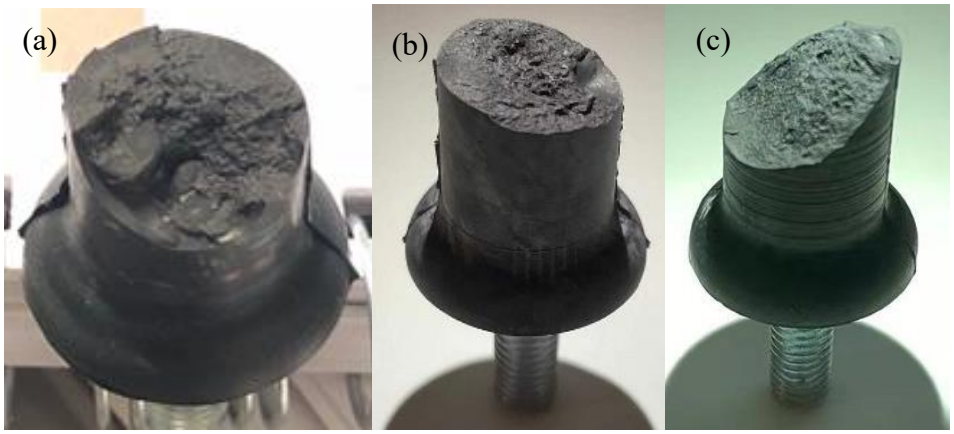

Figure 4.18: Side view of the fracture surface of a sample at (a) 20 ℃, (b) 50 ℃, and (c) 80 ℃.

4.2.4 Size effect

Although the experimental requirements were the same, the crack propagation phenomena for rubber samples of different sizes looked different (Figure 4.19). The fracture surface of the small sample was relatively flat and perpendicular to the direction of the force, that is, the direction of crack propagation was perpendicular to the direction of the force. But its fracture surface did not have the third stage — brittle fracture. The fracture surface of the small sample was more similar to that of the reference test sample at low frequency or low amplitude, as it was full of stripes and had relatively average roughness.

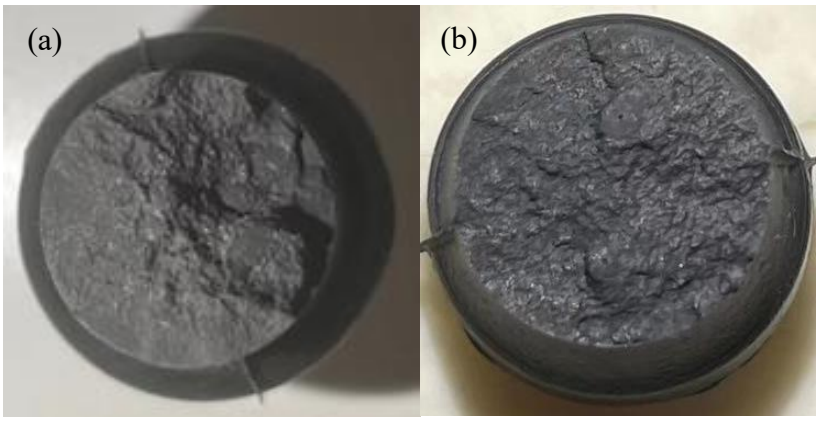

Figure 4.19: Top view of fracture surface of (a) reference sample and (b) small sample.

4.2.5 Aging effect

4.2.5.a Thermal aging

Figure 4.20 shows the fracture surface of all aging conditions. For the sample aged 2 days, the fracture surface can be divided into three zones. After the microcracks appeared on the

surface, they gradually expanded from left to right. The surface with stripes, on the left, was rough, and the one on the right was smooth. This is because the final brittle fracture occurred in the sample, and thus the final fracture surface was smooth. This crack propagation method is the same as it was for the aged sample.

The fracture surface of the sample aged for 4 days was similar to that of the sample aged for 2 days. However, the difference is that the sample aged for 4 days had a smooth, narrow ring near the sample surface. The area inside the ring exhibited a typical crack propagation pattern.

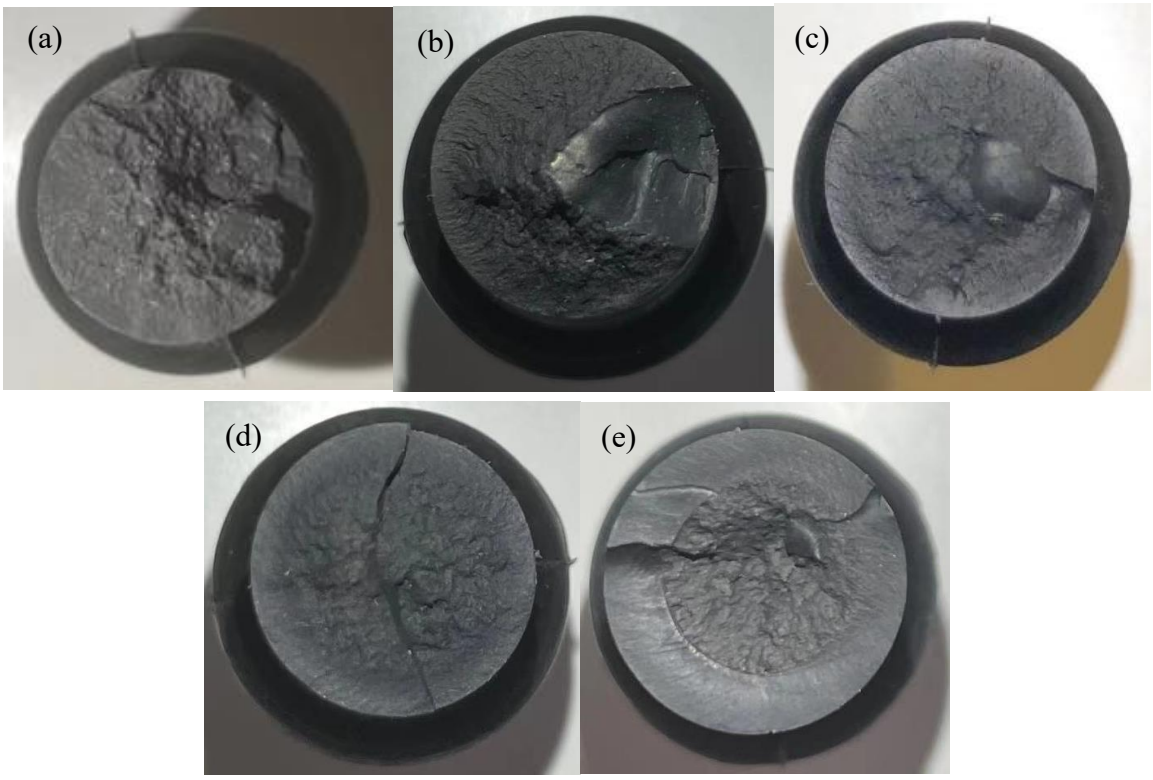

Figure 4.20: Fracture surface of (a) unaged sample and samples aged for (b) 2 days, (c) 4 days, (d) 8 days, and (e) 16 days.

According to the fatigue curve of the sample mentioned in section 4.1.5.a, the fatigue failure process of the samples aged for 8 days and 16 days was completely different from that of the reference experimental group. After a long thermal aging treatment, the chemical and physical properties of the rubber sample had changed. From a macro point of view, after 8 days of heat aging, the surface of the sample becomes harder and its elasticity also worsens. When the tensile test was carried out, multiple cracks immediately appeared on the surface of the sample, which at that point became a brittle fracture. The appearance of the fracture interface is the ring close to the surface of the sample. The fracture section inside the ring also showed similar fatigue crack propagation progress.

This feature looks clearer on the fracture surface of samples aged 16 days. In other words, the crack propagation direction is from the edge of the sample to the centre. According to Charrier et. al [39], this phenomenon is due to the diffusion limited oxidation (DOL) effect, resulting in a sharp aging profile.

For the samples aged for 8 and 16 days, their elasticity is reduced owing to the change in chemical properties, and these samples are no longer suitable for use.

4.2.5.b Liquid aging

According to Figure 4.21, a sample immersed in the reference liquid and the sample not immersed showed the same fatigue crack propagation progress. Even if the length of

immersion in the liquid was different, it did not have a significant effect on the chemical properties and fatigue aging properties of the sample.

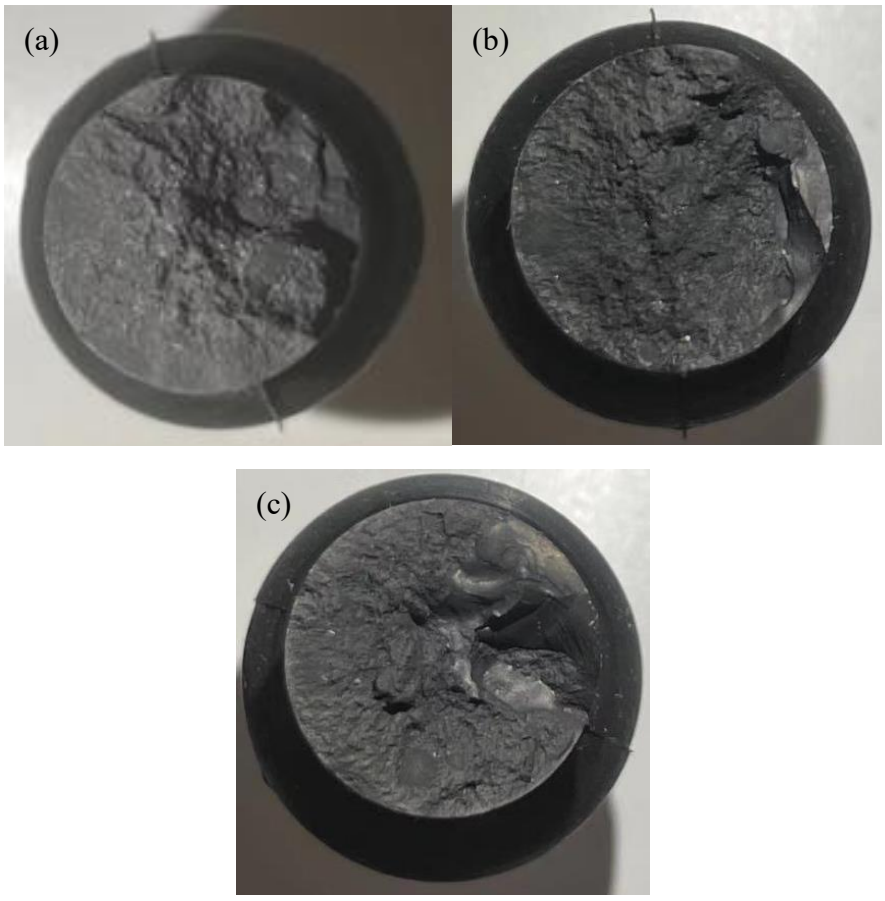

Figure 4.21: Fracture surface of (a) unaged sample and samples aged for (b) 70h and (c) 166h.

Chapter 5: Conclusion and Future Work

In this final chapter, a summary of conclusion from each chapter is presented and proposes requirements and ideas for future work.

5.1 Conclusion

The purpose of this article is to explore the influence of external factors on the fatigue life of natural rubber and the process of the macroscopic crack growth. The general conclusion can be summarized as follow:

1. The rubber undergoes three stages from fatigue to failure under uniaxial tension. The first stage is stress softening leading to a decrease in load. The second stage is when the load enters a plateau, and internal microscopic cracks are formed. The third stage is the formation of macroscopic cracks on the surface of the sample. As the cracks growth, the sample will eventually break completely.
2. The rubber fracture section is divided into three parts: the crack initial zone, the crack propagation zone and the brittle fracture zone.
3. The initial zone of the crack is close to the surface of the sample, relatively flat and small. The crack expansion area is larger, the surface is covered with stripes and is getting rougher and rougher. The final brittle fracture zone is very smooth.

4. With the increase of the deformation, the fatigue life of natural rubber decreases, and the more heat generated by the self-heating effect, the higher the surface temperature of the rubber sample.
5. When the deformation amount is 25%, the fracture surface of the sample is flat and there is no third brittle fracture zone. When the amount of deformation increases, the brittle fracture zone appears on the surface of the sample.
6. Below 5 Hz, as the frequency increases, the fatigue life of the rubber increases, and the fracture surface without brittle fracture zone. When the frequency exceeds 5 Hz, as the frequency increases, the fatigue life of the rubber sample decreases, and the brittle fracture shows on the fracture surface.
7. As the frequency increases, the heat generated by the self-heating effect of rubber also increases, making the surface temperature of the rubber higher. The time for the surface temperature of the sample reach to certain degree and remain stable is almost the same.
8. As the temperature increases, the fatigue life of the rubber decreases, and the area of the brittle fracture zone of the fracture surface increases, and the crack propagation direction is not perpendicular to the load direction.
9. For dumbbell-shaped short rubber samples, the cracks occurred at the smallest diameter of the middle sample. The fractured surface is flat and covered with stripes.
10. Thermal aging has a greater impact on the fatigue life of rubber. When the aging time is within 4 days, although the fatigue life is reduced, the complete fatigue failure

process can be maintained. When the heat aging time exceeds 4 days, the physical properties of the rubber will change, become hard and lose its elasticity. The fatigue life is greatly reduced, so it also cannot be in use.

11. Liquid aging has almost no effect on rubber aging life. The fracture cross-section is similar to that of the unaged sample without any significant difference.
12. When the deformation, frequency, and temperature increase, the fatigue life of the rubber decreases, the fracture section is rugged, the crack propagation direction is no longer perpendicular to the load direction, and the brittle fracture zone becomes larger.

5.2 Future work

Although the results of this work can be used to provide information for the future design, production and application of rubber components, which can appropriately prevent or delay the appearance of rubber fatigue, there are many aspects that can be further explored. Suggested next research steps ar1.e as follows:

1. Perform the experiment at negative temperature and compare the fatigue performance with the experimental results at positive temperature. Observe the similarities and differences of the fractured sections.
2. Observe the formation of microscopic cracks and the way and the direction of crack propagation through X-ray CT scanning.

3. Observe the microscopic characteristics of the fractured surface by Scanning Electron Microscope and explore the different or typical characteristics of microscopic cracks under the influence of external factors.

References

[1] Choi, J.H., Kang, H.J., Jeong, H.Y., Lee, T.S., and Yoon, S.J., 2005, "Heat aging effects on the material property and the fatigue life of vulcanized natural rubber, and fatigue life prediction equations," Journal of Mechanical Science and Technology (KSME International Journal), Vol. 19, No. 6, pp. 1229-1242.

[2] Zhang, Z., Sun, J., Lai, Y., Wang, Y., Liu, X., Shi, S., & Chen, X. (2018). Effects of thermal aging on uniaxial ratcheting behavior of vulcanised natural rubber. *Polymer Testing*, 70, 102-110.

[3] Mars W V,Fatemi A. Fatigue crack nucleation and growth in filled natural rubber. *Fatigue and Fracture of Engineering Materials and Structures*,*2003*,*26*(9):779-789.

[4] Moon S I,Cho I J,Woo C S,et al. Study on determination of durability analysis process and fatigue damage parameter for rubber component. *Journal of Mechanical Science and Technology*,*2011*,*25*(5), 1159-1165.

[5] Mars W V,Fatemi A. Multiaxial fatigue of rubber part I: equivalence criteria and theoretical aspects. *Fatigue Fracture Engineer Material Structure*,*2005*,*28*(6), 515-522.

[6] Cruanes, C., Lacroix, F., Berton, G., Meo, S., and Ranganathan, N. (2015). Study of the Fatigue Behavior of a Synthetic Rubber Undergoing Cumulative Damage Tests.

International Journal of Fatigue, 91 (2016), 322-327. doi: https://doi.org/10.1016/j.ijfatigue.2015.11.026.

[7] Le Cam, J-B., & Toussaint, E. (2010). The Mechanism of Fatigue Crack Growth in Rubbers under Severe Loading: the Effect of Stress-Induced Crystallization. *Macromolecules, 2010, 43* (10), p4708-4714. https://doi.org/10.1021/ma100042n

[8] Beilen, J., & Poirier, Y. (2007). Establishment of new crops for the production of natural rubber. *Trends in Biotechnology, Vol25* (11). doi:10.1016/j.tibtech.2007.08.009

[9] Hamilton, J. L. (2016). *Natural Rubber: Properties, Behavior and Applications.* Nova Science Publishers.

[10] Mooibroek, H., & Cornish, K. (1999). Alternative sources of natural rubber. *Applied Microbiology and Biotechnology, 2000* (53), p355-365. https://doi.org/10.1007/s002530051627

[11] Schaefer, R. J. (2010). Mechanical properties of rubber. *Harris' Shock and Vibration Handbook, Sixth edition, A. Piersol, T. Paez (Eds), McGraw-Hill Companies Inc*, 33-1.

[12] Henneberry, B. All about natural rubber - properties, applications and uses. Retrieve from https://www.thomasnet.com/articles/plastics-rubber/all-about-natural-rubber-properties-applications-and-uses/

[13] Mars, W., Fatemi, A. (2002). A Literature Survey on Fatigue Analysis Approaches for Rubber. *International Journey of Fatigue, 24* (9), 949- 961.

[14] André, N., Cailletaud, G., & Piques, R. (1999). Haigh diagram for fatigue crack initiation prediction of natural rubber components. *Kautschuk Gummi Kunststoffe, 52*(2), 120-123.

[15] Roberts, B. J., & Benzies, J. B. (1977). The relationship between uniaxial and equibiaxial fatigue in gum and carbon black filled vulcanizates. *Proceedings of rubbercon, 77*(2), 1-13.

[16] Gent, A. N., Lindley, P. B., & Thomas, A. G. (1964). Cut growth and fatigue of rubbers. I. The relationship between cut growth and fatigue. *Journal of Applied Polymer Science, 8*(1), 455-466.

[17] Griffith, A. A. (1921). VI. The phenomena of rupture and flow in solids. *Philosophical transactions of the royal society of london. Series A, containing papers of a mathematical or physical character, 221*(582-593), 163-198.

[18] Mullins, L. (1958). Rupture of rubber. IX. Role of hysteresis in the tearing of rubber. *Transactions of the Institution of the Rubber Industry, 35*(5), 213-222.

[19] Diani, J., Fayolle, B., & Gilormini, P. (2009). A review on the Mullins effect. *European Polymer Journal, 45*(3), 601-612.

[20] Lindley, P. B. (1973). Relation between hysteresis and the dynamic crack growth resistance of natural rubber. *International Journal of Fracture, 9*(4), 449-462.

[21] Le Cam, J. B., & Toussaint, E. (2008). Volume variation in stretched natural rubber: competition between cavitation and stress-induced crystallization. *Macromolecules, 41*(20), 7579-7583.

[22] Woo, C. S., Kim, W. D., & Kwon, J. D. (2008). A study on the material properties and fatigue life prediction of natural rubber component. *Materials Science and Engineering: A, 483,* 376-381.

[23] Schieppati, J., Schrittesser, B., Wondracek, A., Robin, S., Holzner, A., & Pinter, G. (2018). Impact of temperature on the fatigue and crack growth behavior of rubbers. *Procedia Structural Integrity, 13,* 642-647.

[24] Flamm, M., Steinweger, T., & Weltin, U. (2002). Cumulative damage in rubber materials. *Kautschuk Gummi Kunststoffe, 55*(12), 665-668.

[25] Le Saux, V., Marco, Y., Calloch, S., Charrier, P., & Taveau, D. (2013). Heat build-up of rubber under cyclic loadings: Validation of an efficient demarch to predict the temperature fields. *Rubber Chemistry and Technology, 86*(1), 38-56.

[26] Cadwell, S. M., Merrill, R. A., Sloman, C. M., & Yost, F. L. (1940). Dynamic fatigue life of rubber. *Rubber Chemistry and Technology, 13*(2), 304-315.

[27] Fielding, J. H. (1943). Flex life and crystallization of synthetic rubber. *Industrial & Engineering Chemistry, 35(*12), 1259-1261.

[28] Beatty, J. R. (1964). Fatigue of rubber. *Rubber Chemistry and Technology, 37*(5), 1341-1364.

[29] Lindley, P. B. (1973). Relation between hysteresis and the dynamic crack growth resistance of natural rubber. *International Journal of Fracture, 9*(4), 449-462.

[30] LE CAM, J. B., Huneau, B., & Verron, E. (2008). Description of fatigue damage in carbon black filled natural rubber. *Fatigue & Fracture of Engineering Materials & Structures, 31*(12), 1031-1038.

[31] Spreckels, J., Weltin, U., Flamm, M., Steinweger, T., & Brüger, T. (2012). Investigations regarding environmental effects on fatigue life of natural rubber. *Constitutive Models for Rubber VII*, 369-374.

[32] Lake, G. J., & Thomas, A. G. (1981). Mechanics of fracture of rubber-like materials. *In Proceedings of the IUTAM Symposium on Finite Elasticity* (pp. 25-45). Springer, Dordrecht.

[33] Shi, X., Ma, M., Lian, C., & Zhu, D. (2013). Investigation on effects of dynamic fatigue frequency, temperature and number of cycles on the adhesion of rubber to steel cord by a new testing technique. *Polymer testing, 32*(6), 1145-1153.

[34] Ruellan, B., Le Cam, J. B., Jeanneau, I., Canévet, F., Mortier, F., & Robin, E. (2019). Fatigue of natural rubber under different temperatures. *International Journal of Fatigue, 124*, 544-557.

[35] Ngolemasango, F. E., Bennett, M., & Clarke, J. (2008). Degradation and life prediction of a natural rubber engine mount compound. *Journal of applied polymer science, 110*(1), 348-355.

[36] Wu, J., Chen, L., Li, H. H., Su, B. L., & Wang, Y. S. (2018, July). Effect of Temperature on Tensile Fatigue Life of Natural Rubber. *In IOP Conference Series: Materials Science and Engineering* (Vol. 389, No. 1, p. 012024). IOP Publishing.

[37] Tee, Y. L., Loo, M. S., & Andriyana, A. (2018). Recent advances on fatigue of rubber after the literature survey by Mars and Fatemi in 2002 and 2004. *International Journal of Fatigue, 110*, 115-129.

[38] Ali, A., Hosseini, M., & Sahari, B. B. (2010). Heat-aging effects on tensile properties of vulcanized natural rubber. *SMR, 10*, 100.

[39] Charrier, P., Marco, Y., Le Saux, V., & Ranaweera, R. K. P. S. (2012). On the influence of heat ageing on filled NR for automotive AVS applications. *Constitutive Models for Rubber VII*, 381-388.

[40] Blackman, E. J., & McCall, E. B. (1970). Relationships between the structures of natural rubber vulcanizates and their thermal and oxidative aging. *Rubber chemistry and technology, 43*(3), 651-663.

[41] Le Gac, P. Y., Arhant, M., Davies, P., & Muhr, A. (2015). Fatigue behavior of natural rubber in marine environment: Comparison between air and sea water. *Materials & Design (1980-2015), 65*, 462-467.

[42] Seichter, S., Archodoulaki, V. M., Koch, T., Holzner, A., & Wondracek, A. (2017). Investigation of different influences on the fatigue behaviour of industrial rubbers. *Polymer Testing, 59*, 99-106.

Appendices

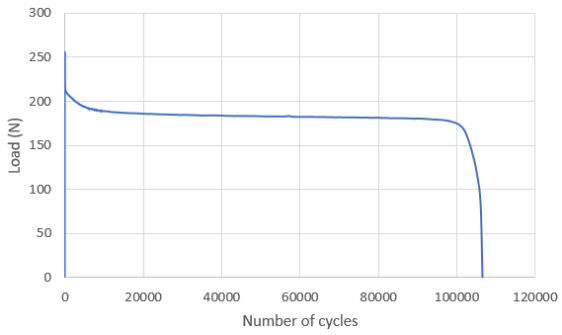

(a)

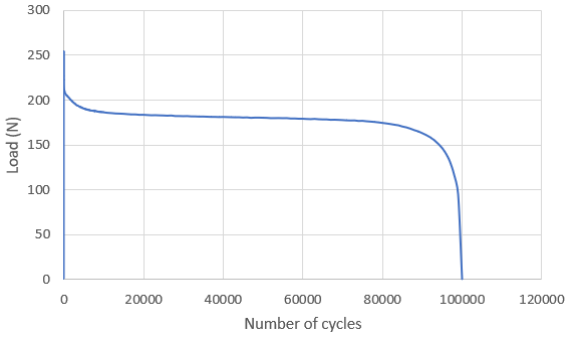

(b)

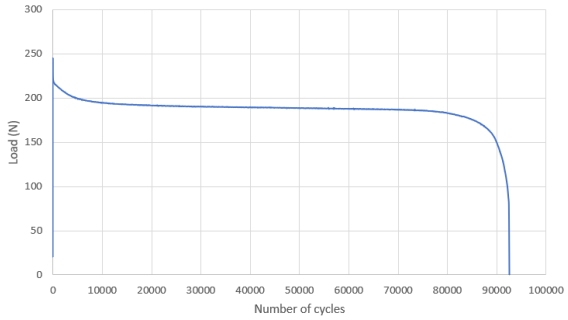

(c)

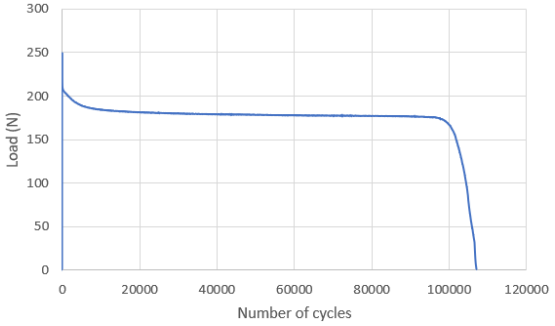

(d)

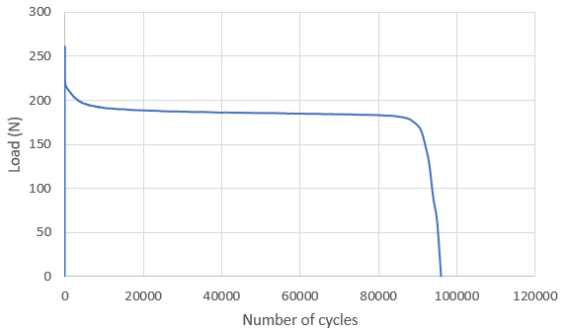

(e)

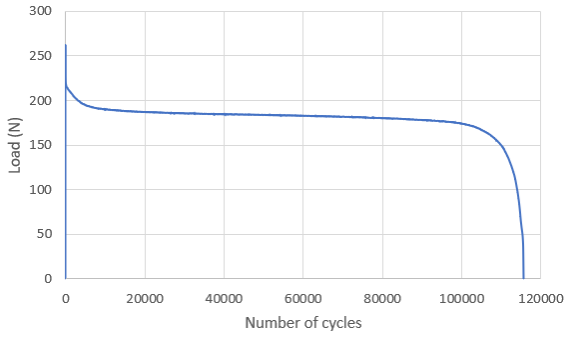

(f)

Appendix 1: References experiment data - 50% strain level, 23 °C, 10Hz.

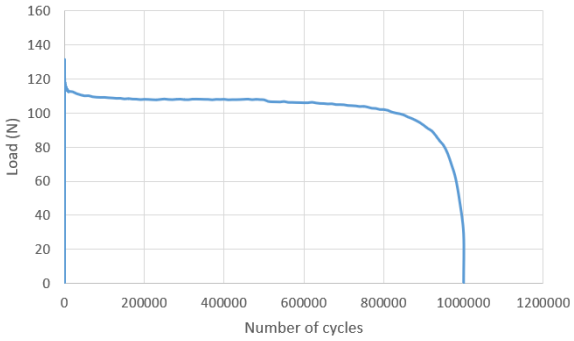

(a)

Appendix 2 : Deformation of 25% experiment data - 23 °C, 10Hz.

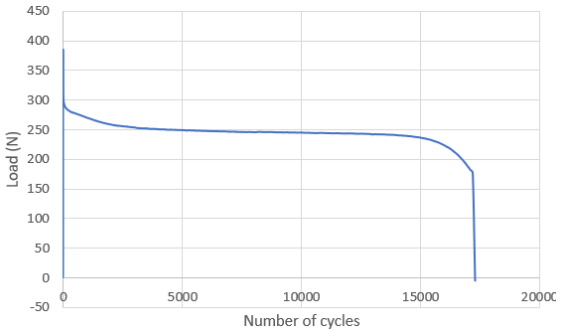

(a)

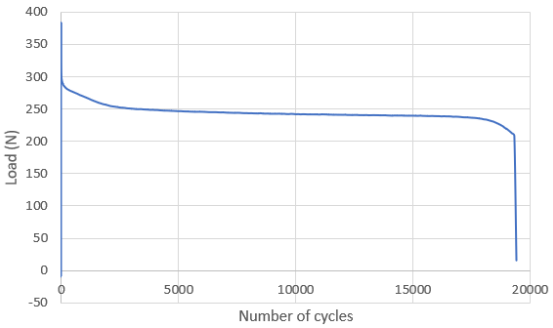

(b)

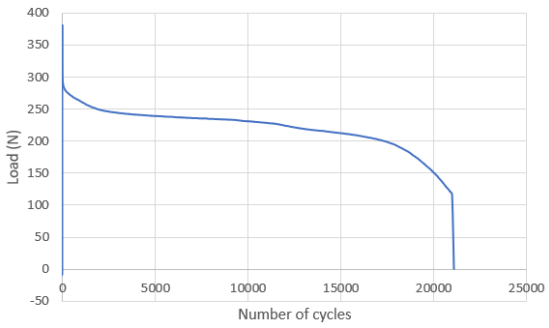

(c)

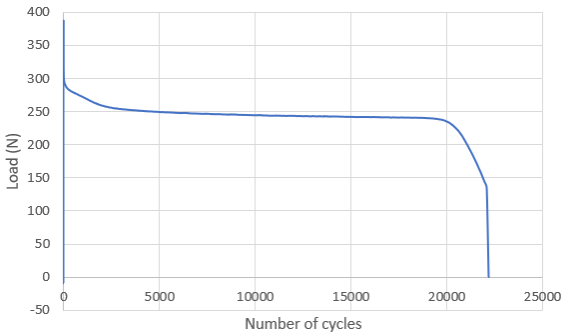

(d)

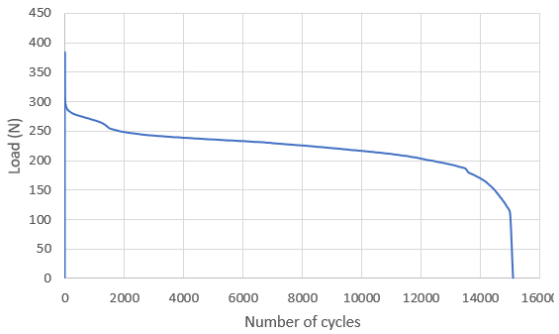

(e)

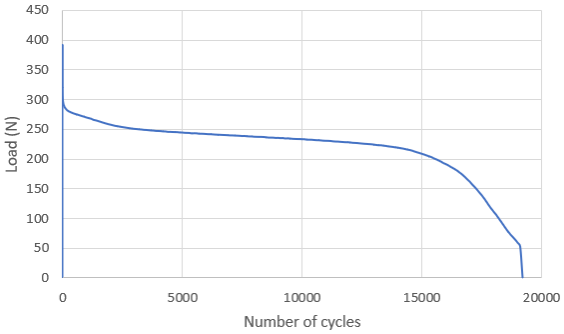

(f)

Appendix 3: Deformation of 75% experiment data - 23 °C, 10Hz.

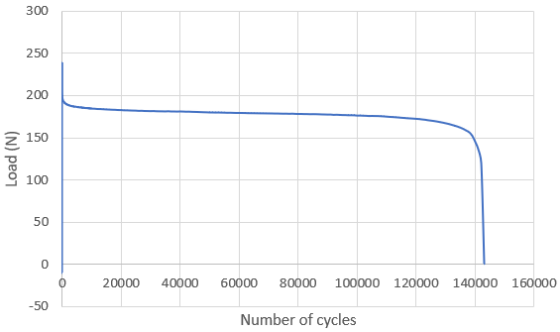

(a)

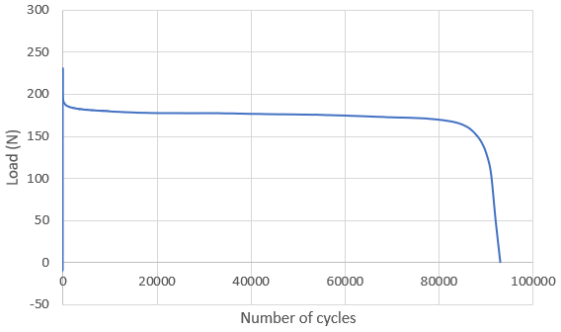

(b)

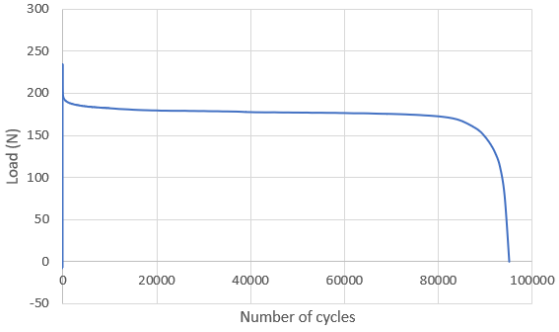

(c)

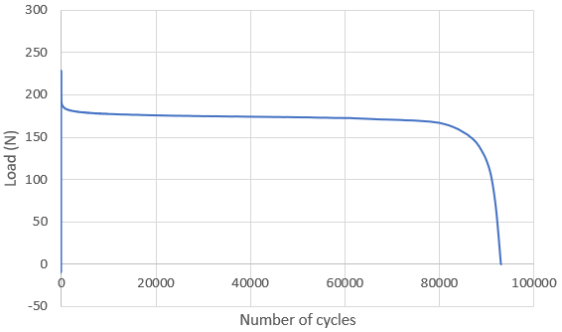

(d)

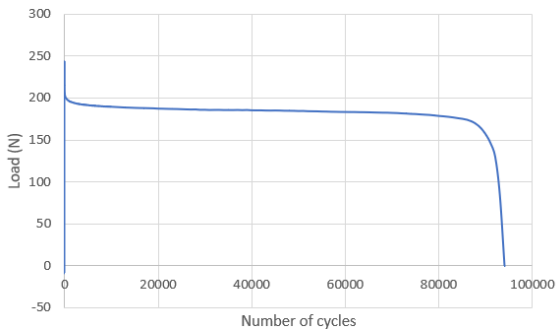

(e)

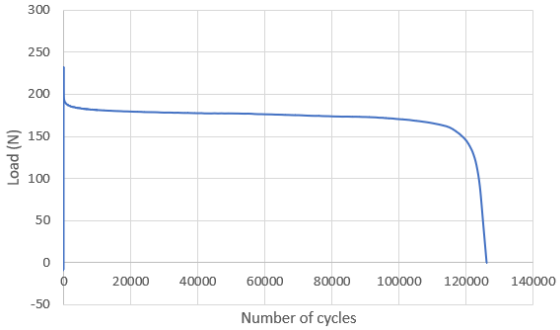

(f)

Appendix 4: Frequency of 1Hz experiment data - 50% strain level, 23 °C.

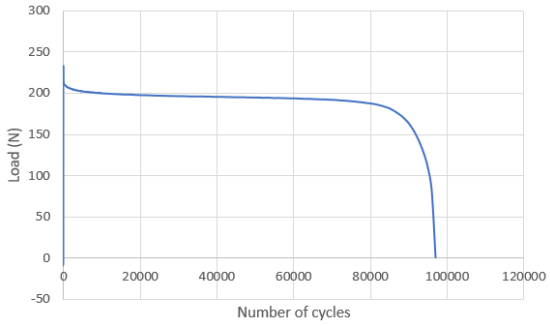

(a)

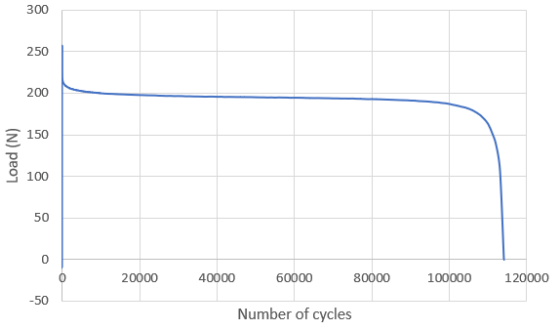

(b)

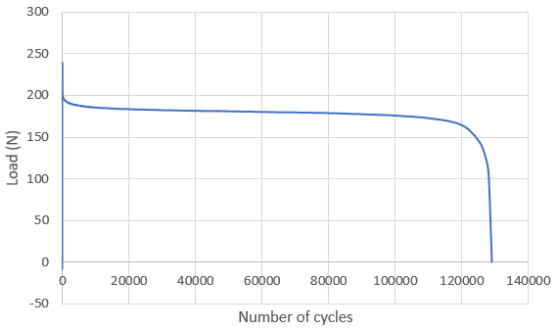

(c)

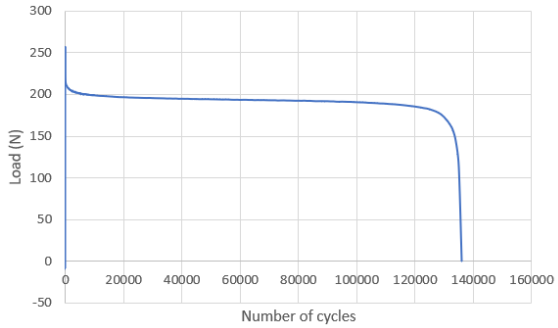

(d)

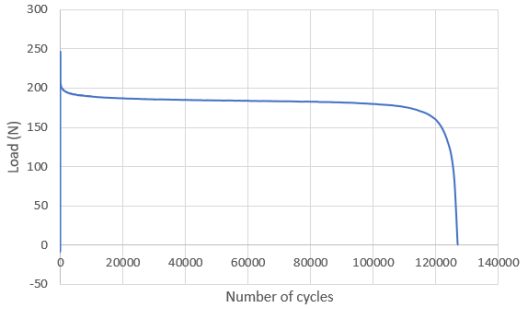

(e)

Appendix 5: Frequency of 2.5Hz experiment data - 50% strain level, 23 °C.

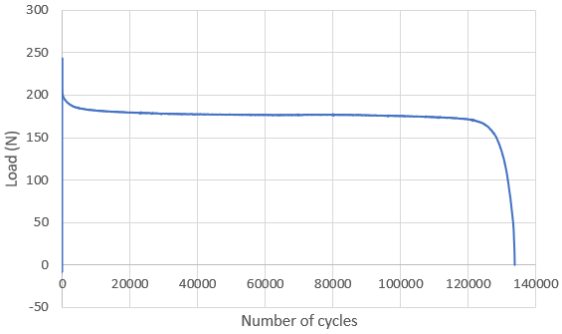

(a)

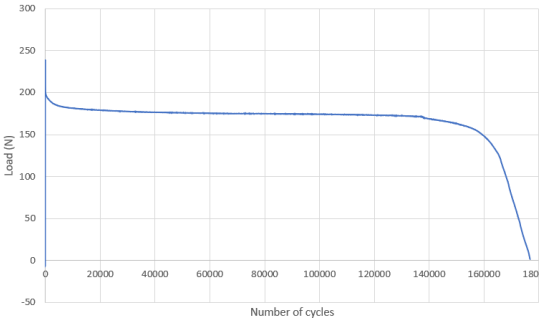

(b)

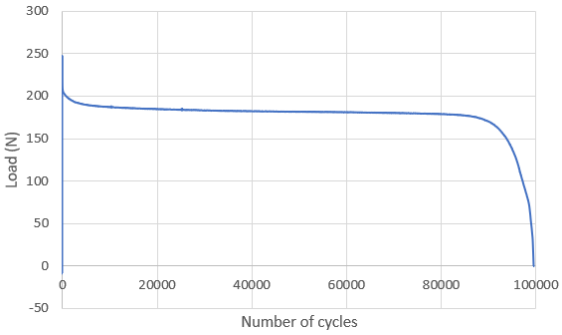

(c)

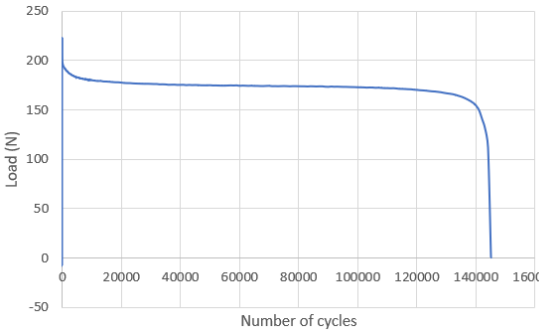

(d)

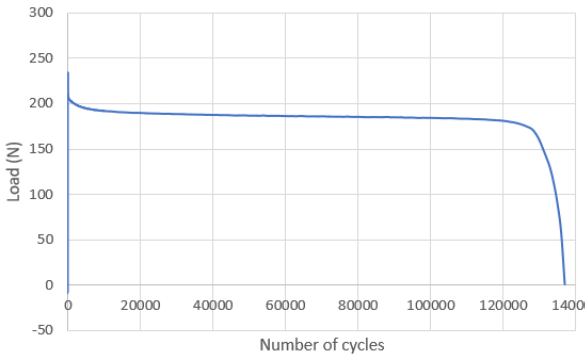

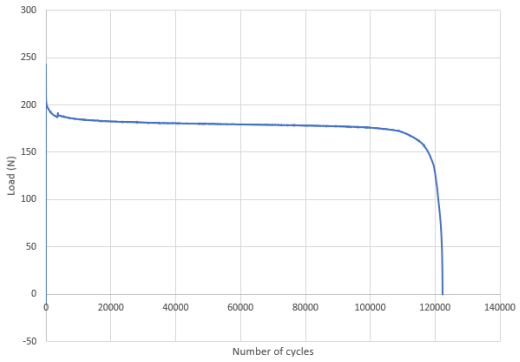

(e) (f)

Appendix 6: Frequency of 5Hz experiment data - 50% strain level, 23 °C.

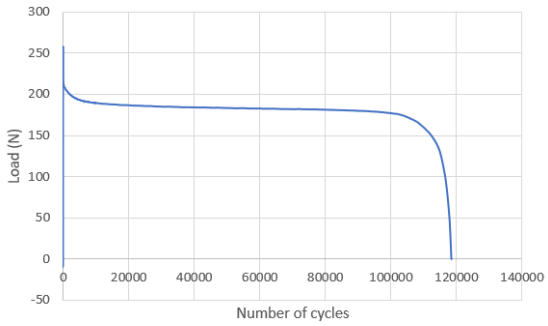

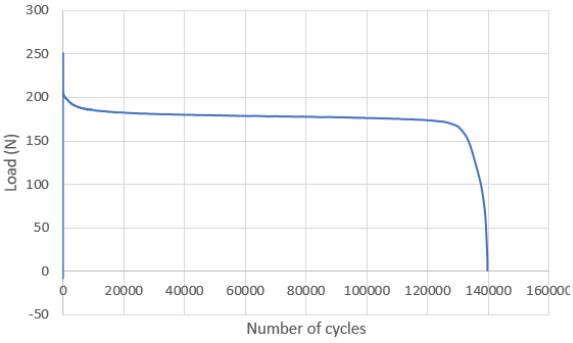

(a) (b)

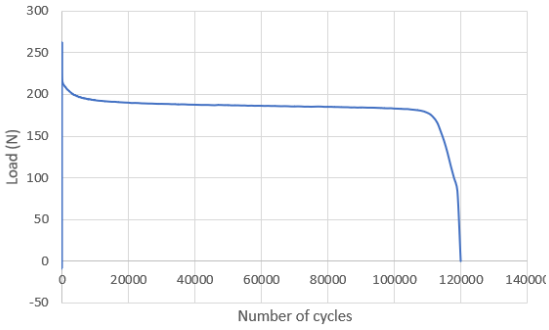

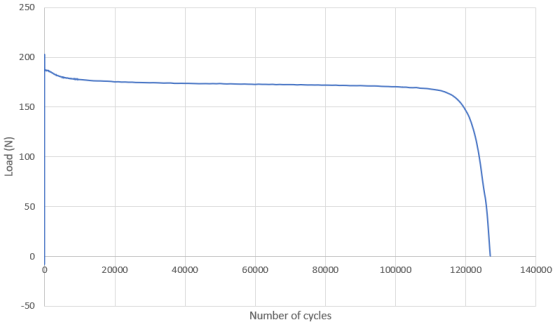

(c) (d)

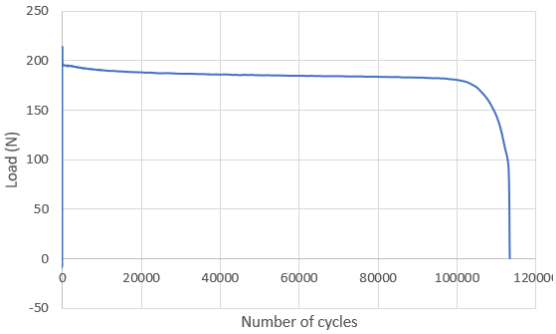

(e)

Appendix 7: Frequency of 7.5Hz experiment data - 50% strain level, 23 °C.

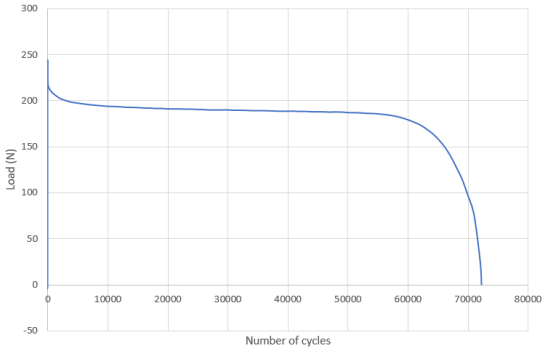

(a)

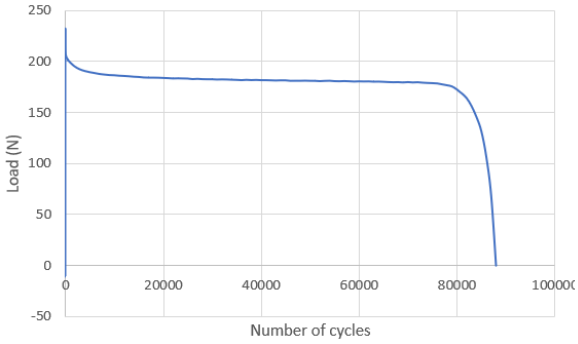

(b)

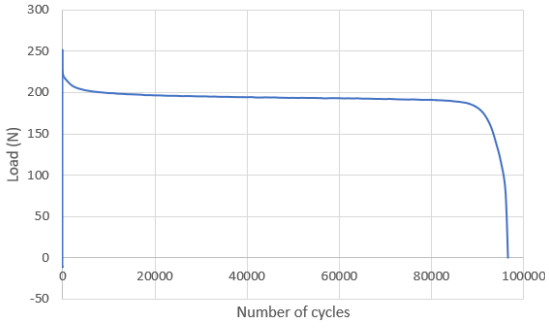

(c)

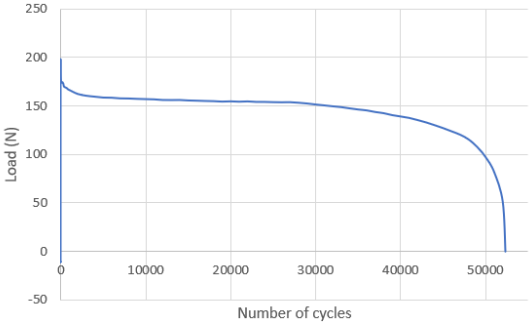

(d)

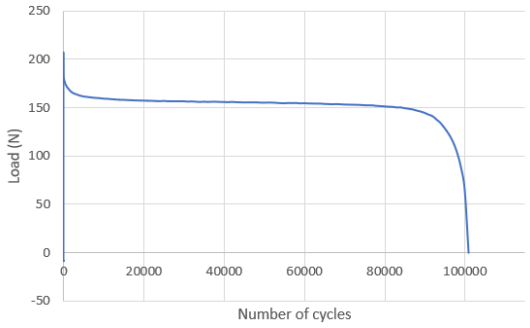

(e)

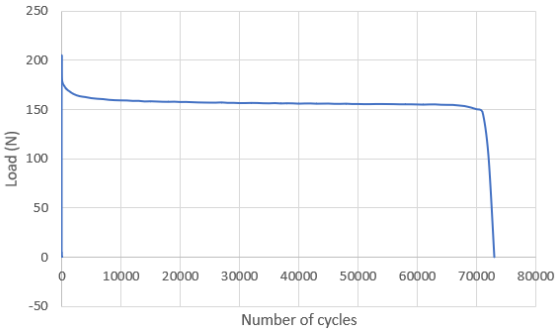

(f)

Appendix 8: Temperature of 50 °C experiment data - 50% strain level, 10Hz.

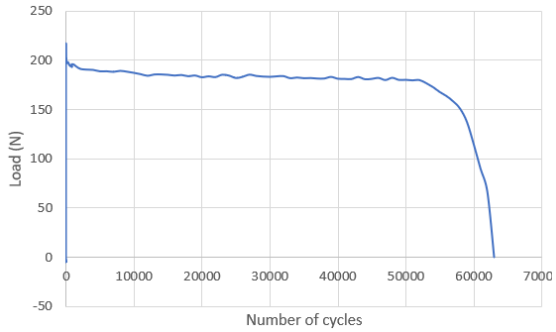

(a)

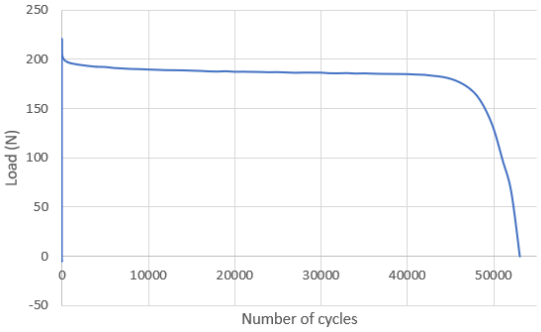

(b)

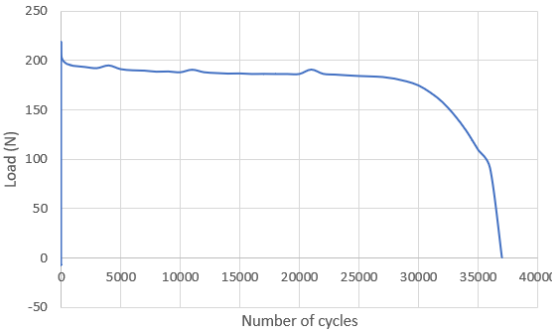

(c)

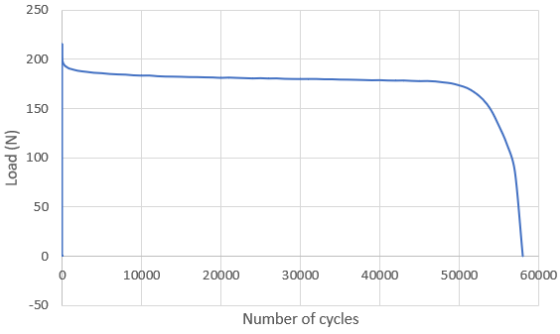

(d)

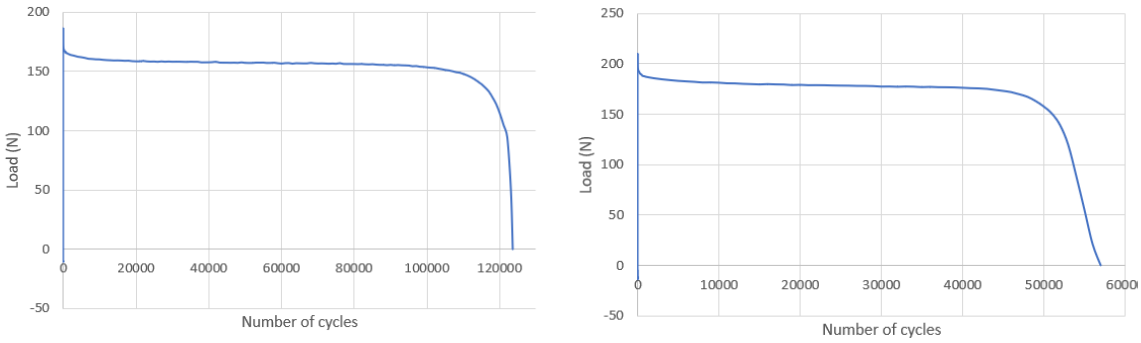

(e) (f)

Appendix 9: Temperature of 80 °C experiment data - 50% strain level, 10Hz.

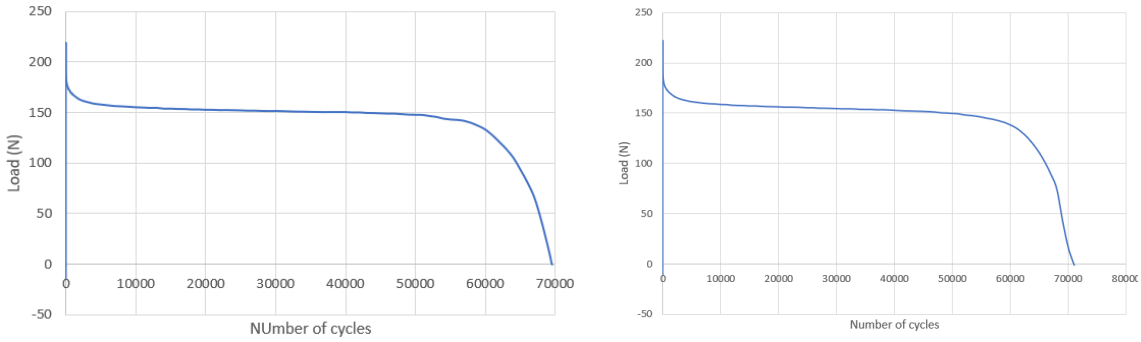

(a) (b)

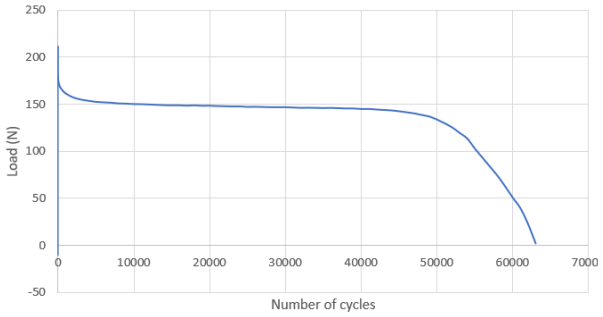

(c)

Appendix 10: Small sample experiment data - 50% strain level, 23 °C, 10Hz.

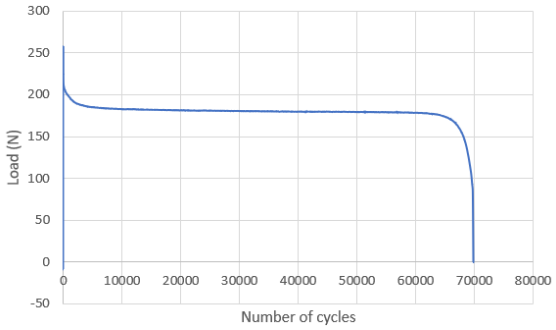

(a)

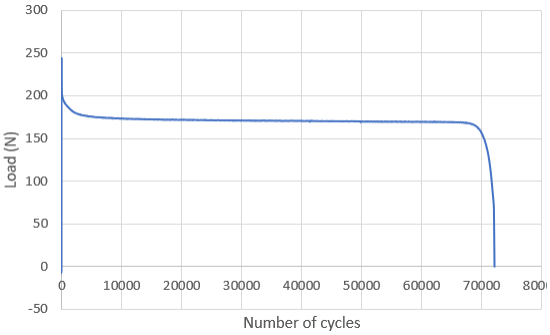

(b)

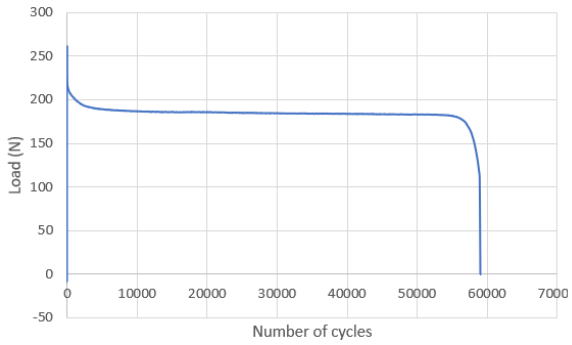

(c)

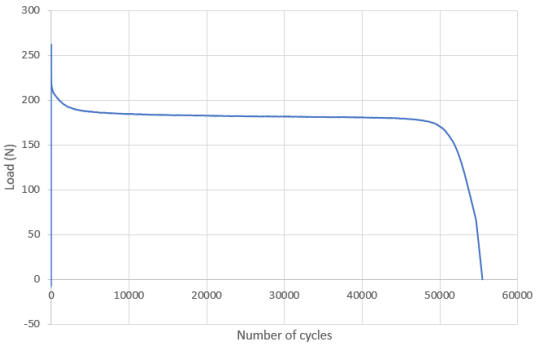

(d)

Appendix 11: 2 days thermal aging experiment data - 50% strain level, 23 °C, 10Hz.

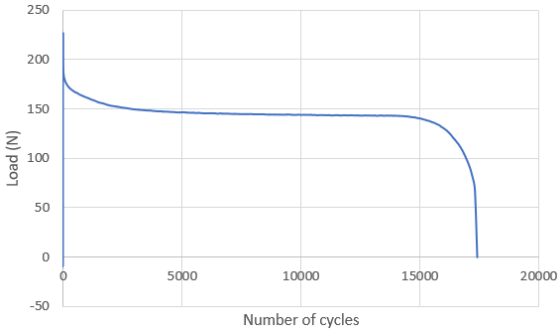

(a)

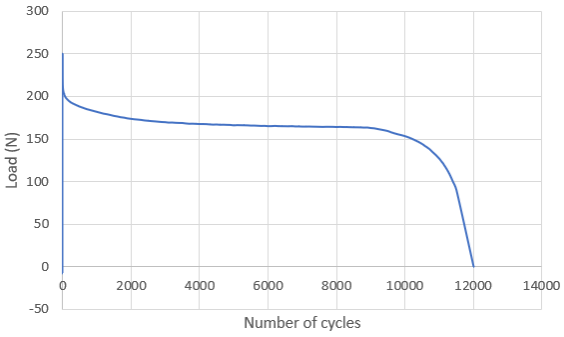

(b)

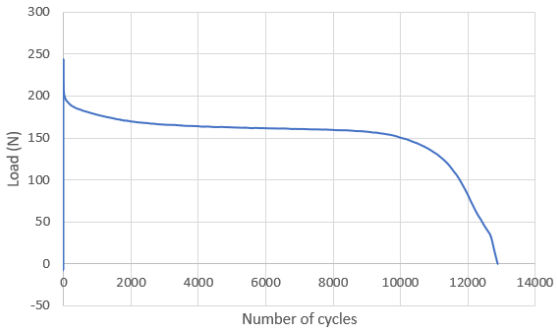

(c)

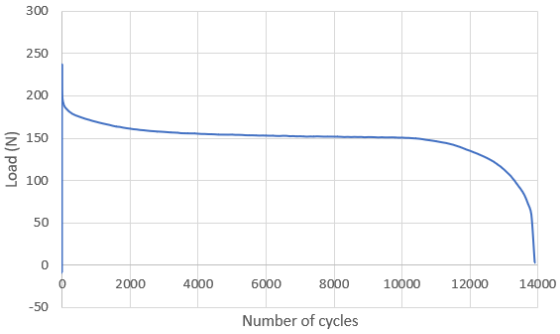

(d)

Appendix 12: 4 days thermal aging experiment data - 50% strain level, 23 °C, 10Hz.

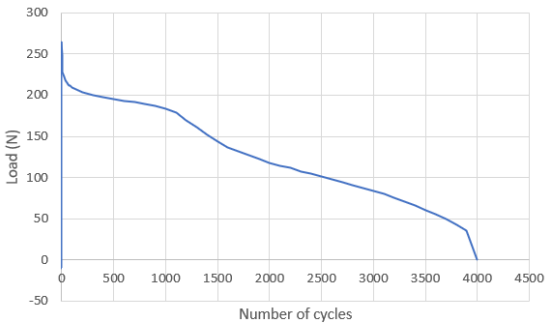

(a)

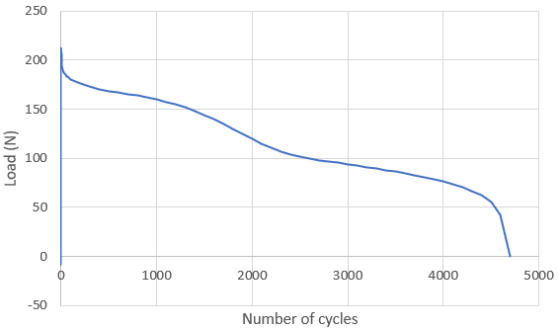

(b)

Appendix 13: 8 days thermal aging experiment data - 50% strain level, 23 °C, 10Hz.

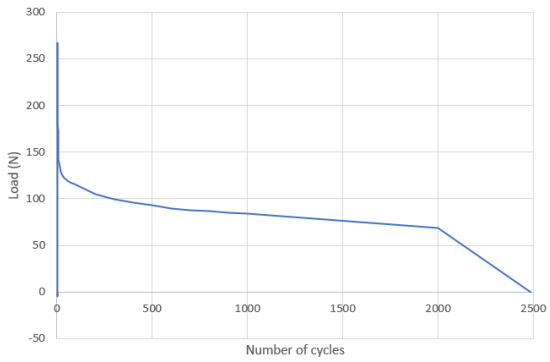

(a)

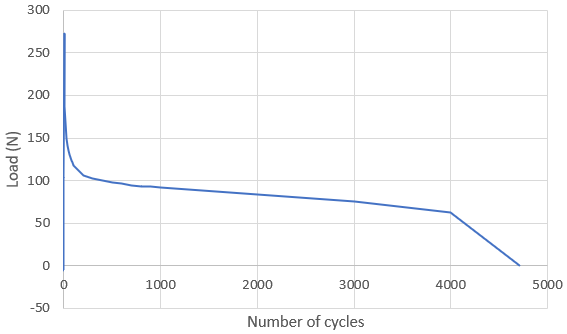

(b)

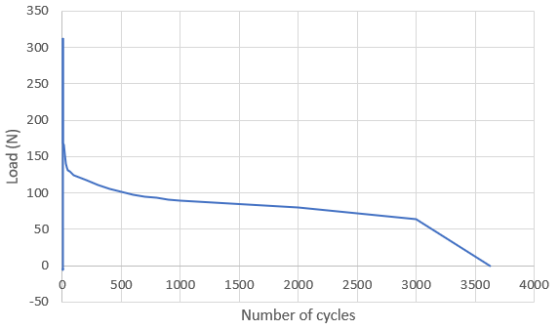

(c)

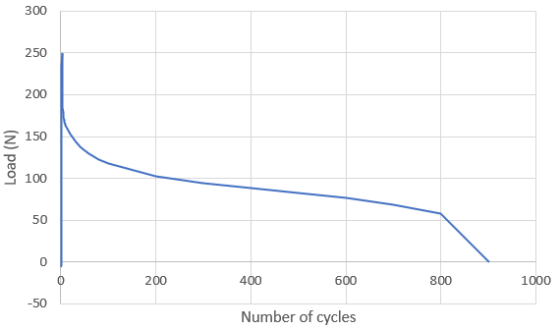

(d)

Appendix 14 : 16 days thermal aging experiment data - 50% strain level, 23 °C, 10Hz.

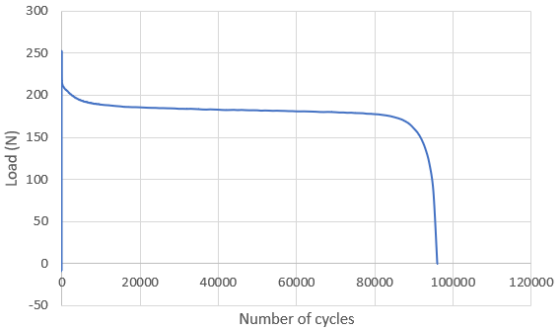

(a)

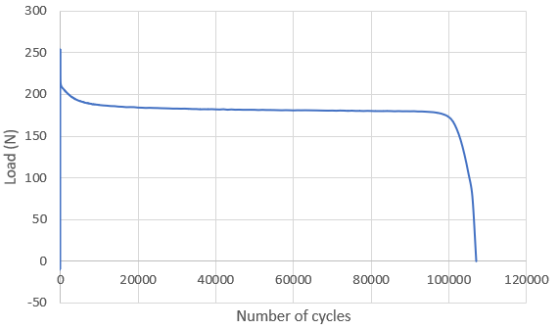

(b)

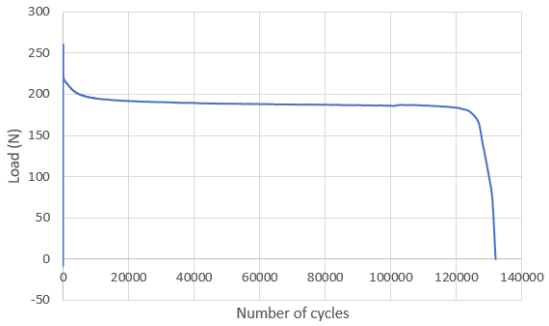

(c)

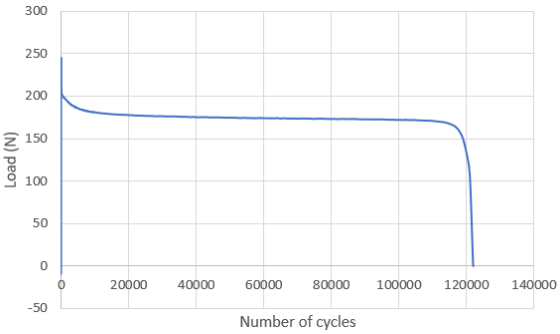

(d)

Appendix 15: 70 hours liquid aging experiment data - 50% strain level, 23 °C, 10Hz.

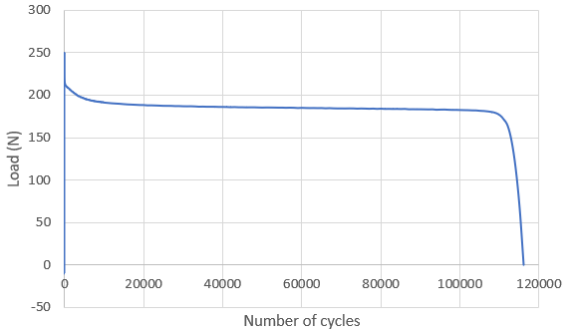

(a)

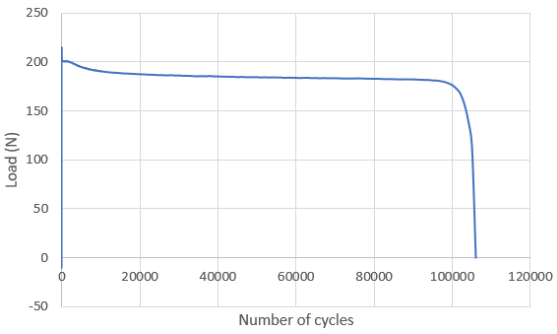

(b)

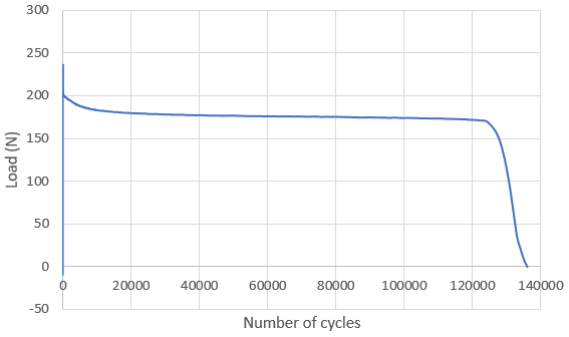

(c)

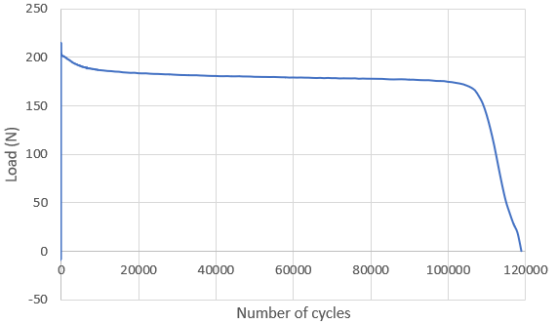

(d)

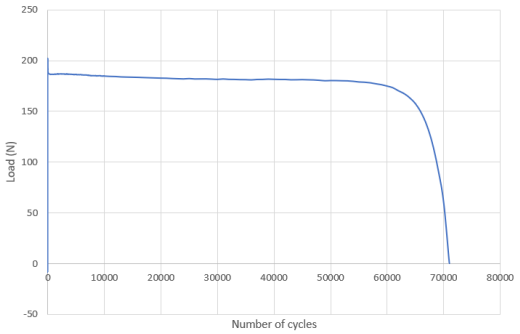

(e)

Appendix 16: 166 hours liquid aging experiment data - 50% strain level, 23 °C, 10Hz.